KICKS AND MAPS
A DIFFERENT APPROACH TO MODELING BIOLOGICAL SYSTEMS

by

Stephen Anthony Ippolito

A Dissertation Submitted to the Faculty of

The Charles E. Schmidt College of Science

in Partial Fulfillment of the Requirements for the Degree of

Doctor of Philosophy

Florida Atlantic University

Boca Raton, FL

December 2015

KICKS AND MAPS

A DIFFERENT APPROACH TO MODELING BIOLOGICAL SYSTEMS

by

Stephen Anthony Ippolito

This dissertation was prepared under the direction of the candidate's dissertation advisor, Dr. Vincent Naudot, Department of Mathematical Science, and has been approved by the members of his supervisory committee. It was submitted to the faculty of the Charles E. Schmidt College of Science and was accepted in partial fulfillment of the requirements for the degree of Doctor of Philosophy.

SUPERVISORY COMMITTEE:

Vincent Naudot, Ph.D.
Dissertation Advisor

Erik Noonburg, Ph.D.

William Kalies, Ph.D.

Tomas Schonbek, Ph.D.

Hongwei Long, Ph.D.

Rainer Steinwandt, Ph.D.
Chair, Department of Mathematical Science

Janet Blanks, Ph.D.
Interim Dean, The Charles E. Schmidt College of Science

Deborah L. Floyd, Ed.D.
Dean, Graduate College

11/23/15
Date

ACKNOWLEDGEMENTS

I wanted to start out by first thanking my Advisor Dr. Naudot for the hours and effort helping me under stand the material and ways to overcoming difficultly in the research and without whose help, guidance and knowledge I would not have completed this dissertation. To Dr. Noonburg for helping me with the biological applications of the mathematics a major theme of my research without whom I would not have been able to conduct my research or dialog with the biological community. For my advisers Dr. William Kalies, Dr. Tomas Schonbek, and Dr. Long, thank you for all of your help both in and outside of the classroom, the discussions, homework assignments, projects ect have been invaluable and are greatly appreciated. Also to Dr. Mireles for helping me prepare for my Preliminary Examination though he is not on my committee and to Dr. Qian for teaching me the practice of statistical modeling. To Dr. Steinwandt and Helen Randal for keeping me on track toward completing my degree.

To my family for all their support and guidance especially my mom.

ABSTRACT

Author:	Stephen Anthony Ippolito
Title:	Kicks and Maps A Different Approach to Modeling Biological Systems
Institution:	Florida Atlantic University
Dissertation Advisor:	Dr. Vincent Naudot
Degree:	Doctor of Philosophy
Year:	2015

Modeling a biological systems, is a cyclic process which involves constructing a model from current theory and beliefs and then validating that model against the data. If the data does not match, qualitatively or quantitatively then there may be a problem with either our beliefs or the current theory. At the same time directly finding a model from the existing data would make generalizing results difficult.

A considerable difficultly in this process is how to specify the model in the first place. There is a need to be practice which accounts for the growing use of mathematical and statistical methods. However, as a systems becomes more complex, standard mathematical approaches may not be sufficient. In the field of ecology, the standard techniques involve discrete maps, and continuous models such as ODE's. The intent of this work is to present the mathematics necessary to study hybrids of these two models, then consider two case studies. In first case we consider a coral reef with continuous change, except in the presence of hurricanes. The results of the data are compared quantitatively and qualitatively with simulation results. For the second case we consider a model for rabies with a periodic birth pulse. Here the analysis is qualitative as we demonstrate the existence of a strange attractor by looking at the

intersections of the stable and unstable manifold for the saddle point generating the attractor. For both cases studies the introduction of a discrete event into a continuous system is done via a Dirac Distribution or Measure.

Dedicated to my parents Karen and Americo Ippolito

KICKS AND MAPS

A DIFFERENT APPROACH TO MODELING BIOLOGICAL SYSTEMS

LIST OF TABLES

LIST OF FIGURES

CHAPTER 1

INTRODUCTION

The intent of this manuscript is to allow for greater and much needed use of mathematics in the biological sciences. A further goal is to articulate clearly the ideas behind the mathematics which are just as important to the biologist as the mathematician. To illustrate an example of why a clear understanding of Mathematical language is important in the scientific process, consider the falling ladder problem commonly given in a first year calculus course. A ladder for of some length is leaning against a wall and the base of the ladder is moving away from the wall at a constant rate. The student is asked how fast the ladder is falling when it has moved some distance. One problem here is that we might also ask students at what point the ladder is falling faster than the speed of light, which stands beyond reason. Here the students begins to set up the problem under the assumption that the Pythagorean Theorem is a good representation of reality. In reality, however, there is a critical time where the ladder looses contact with the wall and the Pythagorean theorem fails to be a good representation. Given the complexity of biological systems compared with a simple ladder problem it is of great importance to clearly understand the mathematical assumptions made. Another example comes from the field of ecology. The assumption is often made that a predator will try to maximize the number of prey consumed per unit time. It sounds clearly started, however if we let E represent the expect value operator then we might mean the predator is trying to maximize $E(X/T)$ or $E(X)/T_{Ave}$ where X is a random variable representing the number of prey consumed, T is a random variable representing time where the next prey is consumed, and T_{ave} is a constant representing the average time between consuming prey. So here

a simple expression has two mathematical expressions each of which is more precise than the original statement, and each extremely different. In the first case, $E(X/T)$, represents a short term maximizer, trying to get the most out of every moment and in the second case $E(X)/T_{Ave}$ represents a long term maximizer where the predator may be willing to go without food for a longer period for a bigger prize in the end.

Being able to precisely state assumptions is what makes mathematics such a powerful tool in the biological sciences. The models are developed with precision mathematically from the current theory, and are tested. As the models are tested the current theory can be expanded, modified or remain the same. The way in which the current manuscript hopes to test in advance the theory is the in the use of implicitly defined dynamical systems and a means of analyzing their dynamics. This manuscript is broken up into four chapters and this introduction. The first two chapters deal with preliminary information of theory in the field of dynamical systems as well as theoretical ecology and epidemiology. The remaining two chapters are based on two case studies employing the preliminary information and implicitly defined maps. The first case study attempts to model the impact of hurricanes on Caribbean coral reefs using an implicitly defined map to allow discrete events such as hurricanes, into an otherwise continuous system. The second case notes that rabies populations often have complex dynamics with impulses. This scenario is modeled using a well known ODE for modeling rabies and is modified as an implicit map to model the pulse like behavior. The resulting dynamics are then studied using least squares regression along cohomological equation for diffeomorphisms.

1.1 CASE STUDIES

Concerning the first of the two case studies mentioned, coral Reefs are important both ecologically and economically and Caribbean reefs have been declining at an exponential rate over the past few decades. Consequently, we need to ask the question

"can the dynamics be changed?" Answering this question is difficult experimentally for reasons both practical and ethical, making mathematical models a reasonable approach. In 2007 a computer simulation was created in [22] to model the impact of hurricanes on Caribbean coral reefs, and understand what the dynamics are. From the simulation an ordinary differential equation model (ODE) was suggested as an analytical representation, and suggested that the reef exhibited a dynamic refereed to as "alternative stable states." To a reader familiar with dynamical systems theory this can also be thought of as a state space with two attracting fixed points. This point is discussed later on in the case study, however for the purposes of the reef what alternative stable states means ecologically is that all things being equal, if we only change the amount of coral or algae in the reef, all other factors remaining the same, the fate of the reef, as coral or algae dominated, be changed. The result of the model answered this question affirmatively. However in answering this question, the continuous ODE model failed to account for discrete events such as hurricanes which impact the reef dynamics. We address the problem using the Dirac Distribution (described in the section on mathematical preliminaries), to account for the discrete even of a hurricane. This addition results in the ODE modeling becoming an implicitly defined dynamical system for which the dynamic are analyzed and bifurcations are studied.

For the second case study the problem of fox rabies in Europe in considered. In Western Europe the problem is under control however at great expense given it is still a large problem in Eastern Europe with the Russian Federation and Ukraine acting as reservoirs. The dynamics are complex and often exhibit pulse behavior due to mating seasons and migration, possible other events. A well knows rabies epidemic model was taken to see if the addition of pulses via the the Dirac Distribution, could exhibit the same type of complex behavior. The resulting dynamics were numerically investigated for chaos.

CHAPTER 2

PRELIMINARIES-MATHEMATICS

2.1 DYNAMICAL SYSTEMS

There are two case studies considered in this manuscript which we have developed models for. In both cases we did not start from scratch but took ODEs which we thought were not sufficient to address the problem they were intended for. A formal definition of an ODE and conditions for uniqueness are given below however a basic understanding of these systems is that of a continuously time varying system specified in terms of its time derivatives.

Definition 1. *[6] Let $J \subseteq \mathbb{R}$,$U \subseteq \mathbb{R}^n$, and $\Lambda \subseteq \mathbb{R}^k$ be open subsets and suppose that $f : J \times U \times \Lambda \to \mathbb{R}^n$ is a smooth function. Here the term "smooth" means that the function f is continuously differentiable. Then an ordinary differential equation (ODE) is an equation of the form*

$$\frac{dx}{dt} = f(t, x, \lambda)$$

Theorem 1. *[6] Consider the initial value problem $f : J \times \Omega \to \mathbb{R}^n$ defined by $\frac{dx}{dt} = f(t, x)$ and $x(0) = x_0$. If f is Lipschitz and continuous with respect to its second argument, then there are open sets $J_0 \subset J$ and $\Omega_0 \subset \Omega$ and a unique continuous function $\sigma : J_0 \times \Omega_0 \to \mathbb{R}^n$ given by $(t, x) \to \sigma(x, t)$ with $t \to \sigma(t, x_0)$ being the unique solution of the initial value problem. In addition if f is C^1 then so is σ*

Our problem with the ODE was precisely the fact that it is continuous as mentioned in the introduction, as we are working with systems that are not continuous

at discrete points in time. Consequently we will work with a model more general than an ODE called a dynamical system which can be thought of as a system with a rule for evolving with time not requiring the system to be discrete or continuous. For studying the dynamics of these systems our main tool will be looking at the stable and unstable manifolds of hyperbolic fixed points. Below we give the definitions for dynamical systems and the stable manifold theorem.

Definition 2. *[25, 28] A dynamical system on E: a C^1 - map*

$$\phi : \mathbb{R} \times E \to E$$

where E is an open subset of $\mathbb{R}^n$ and if $\phi_t(x) = \phi(t, x)$ then ϕ_t satisfies the following properties.

- $\phi_0(x) = x$ *for all* $x \in E$
- $\phi_t \circ \phi_s(x) = \phi_{t+s}(x)$ *for all* $t, s \in \mathbb{R}$ *and* $x \in E$

Theorem 2. *[25, 28] Stable Manifold Theorem for Maps:*
Let $P : \mathbb{R}^n \to \mathbb{R}^n$ be a C^1- diffeomorphism with a hyperbolic fixed point $0 \in \mathbb{R}^n$. Then there exists local stable and unstable invariant manifolds S and U of class C^1 tangent to the stable and unstable subspaces E^s and E^u of $DP(0)$ and of the same dimension such that for all $x \in S$ and $n \geq 0$, $P^n(x) \in S$ and $P^n(x) \to 0$ as $n \to \infty$ and for all $x \in U$ and $n \geq 0$, $P^{-n}(x) \in U$ and $P^{-n}(x) \to 0$ as $n \to \infty$

We define the global stable and unstable manifolds respectively as

$$W^s(0) = \bigcup_{n \geq 0} P^{-n}(S)$$
$$W^u(0) = \bigcup_{n \geq 0} P^n(U)$$

It should be noted, however, that if we are working with a diffeomorphism then the differentiability of the stable and unstable manifolds is not restricted to C^1 but

matches the differentiability of P. In this manuscript since we will be working with analytical differomorphisms, then our stable and unstable manifolds will be analytic as well.

2.2 DEMONSTRATING CHAOS

Sufficient for demonstrating the presence of chaos in for a dynamical system is to show the existence of a horseshoe map. This is typically done by locating a transverse intersection of the stable and unstable manifolds for a saddle point of a diffeomorphism. The reasoning for this is illustrated in the Figure 2.1 below. Consider in I the saddle at A with stable and unstable manifolds indicated by the arrows. The intersection of these manifolds at B creates a homoclinic loop with the homoclinic point at B converging toward A as we take iterations forwards or backwards in time. Due to this loop the action of the map on the box in I will stretch, compress and bend the box along the loop as seen in II. When the intersection of the manifolds is transverse, as in the diagram, there exists an integer n such that the map of the composition f^n is conjugate to the horseshoe map and thus contains a chaotic set [28, 25].

The horseshoe map can be understood as follows. Consider the unit square S containing two vertical strips V_1 and V_2, and two horizontal strips H_1 and H_2, with the S extended by sets A and B resulting in a topological disk is in I of the figure below. Now consider a diffeomorphism f defined on the unit square for which $f(H_1) = V_1$, $f(H_2) = V_2$ and $S \cap f^{-1}(S) = H_1 \cup H_2$. Now suppose that V_1 and V_2 are disjoint and separated by a set G, as in I. This map can be achieved by considering f as the composition of two maps. The first map compresses and stretches the unit square, and the second bends the resulting set back into the unit square. The points that intersect H_1 and H_2 are again mapped into V_1 and V_2 resulting in a horseshoe shape as we see in II and again in III. If we consider the vertical lines in S they converge to cantor set crossed with the interval $[0, 1]$. Inverse iterations of f on S converge to

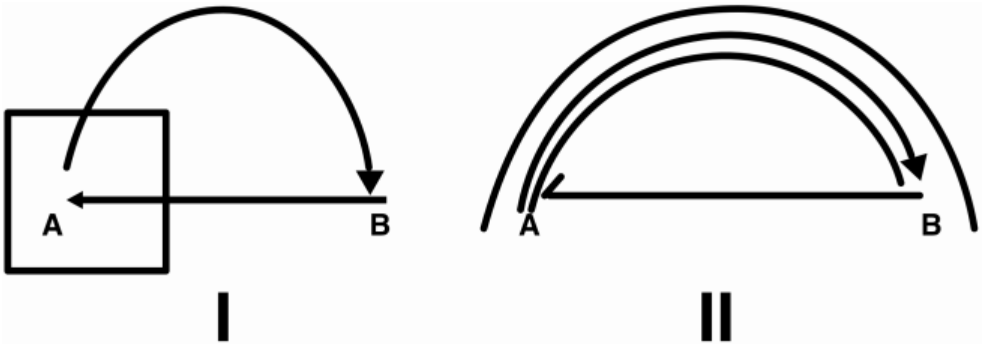

Figure 2.1: A Saddle Point at (A) with homoclinic point at (B) with respect to a map f. If we consider a box around the saddle, the action of f stretches and bends the box toward (B) along the unstable manifold. The stable manifold is pushing points from (B) towards (A) compresses the box. If the intersection of the stable and unstable manifolds at (B) is transverse for some integer n, then the map f^n is conjugate to a horseshoe map and hence contains a periodic orbit.

the interval $[0, 1]$ crossed with a cantor set. Since the cantor set is contained in the interval $[0, 1]$ the intersection of these two sets, which we will call λ is the cross of two cantor sets which is homeomorphic to a cantor set of the line. The set λ contains a chaotic set of the map f. More specific details can be found in [28, 25, 9]

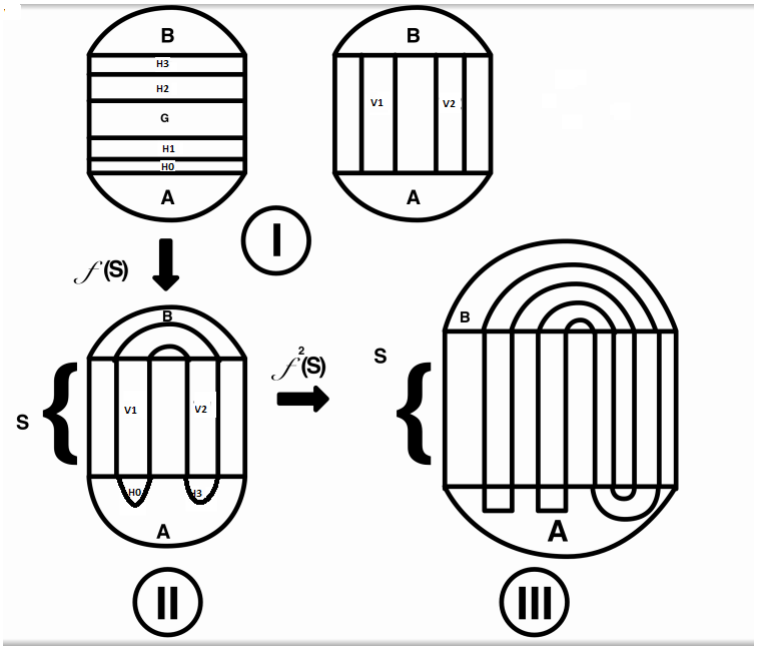

Figure 2.2: The figure above depicts the action of the horseshoe map acting on the unit square as described in the above discussion.

2.3 DIRAC DISTRIBUTION

As previously mentioned we will be working with systems that are combinations of discrete and continuous systems. The combination is done by the use of kicks at discrete times in our ODEs. A kick is added to the ODE through the Dirac distribution δ, defined by the property that

$$\int_{-\infty}^{\infty} f(t)\delta(t)\,dt = f(0) \tag{2.1}$$

for all continuous functions f defined on $\mathbb{R}$. Equivalently δ may be defined as a probability measure that takes the value of 1 for all sets containing the origin and 0 otherwise [9, 17, 27]. Effectively this can be thought of composing the flow of an ODE with another map at some fixed time, on the state space(ODE variables not including time), which will be derived from the Dirac Distribution. Since we can usually not compute the flow explicitly for and ODE we will be working with an implicit map,

and since we are composing this flow with another map due to the kick, we cannot employ techniques used to study differential equations.

CHAPTER 3

PRELIMINARIES - BIOLOGY

The aim of this work is modeling implicit systems and studying their dynamics. Our implicit systems will be hybrids in the sense they involve both continuous and discrete time. For the benefit of the reader here we review the preliminary theory necessary for this objective. First we begin by considering some of the principles of ecological modeling, followed by reviewing the dynamical systems theory necessary to understand the modeling techniques used in the case studies.

3.1 FUNCTIONAL RESPONSE

Ecological models generally consider the interaction of predator and prey. This interaction is generally modeled by what is termed a Functional Response with the following definition.

Definition 3. *Functional Response: The rate at which a predator consumes a prey as a function of prey density or population.*

In general there are three basic types of functional responses referred to as Type I,Type II, and Type III, as given below.

- Type I: $g(H,t) = aH(t)$
- Type II: $g(H,t) = \dfrac{aH(t)}{1 + aT_hH(t)}$
- Type III: $g(H,t) = \dfrac{aH(t)^2}{z + H(t)^2}$

a: *The attack rate* *H*: *Prey population, or density* T_h: *handling time* *t*: *time* *z*: *constant* *g*: *Prey consumed*

The Type I, can be thought of as a special case of the Type II where $T_h = 0$. The Type II, often referred to as Holling Disc Equation assumes a constant handling time, a linear relationship between search time and number of prey encountered and that handling and pursuing prey cannot be done simultaneously. The Type II can be derived as follows.

$$\begin{cases} g &= aT_sH \\ \\ T_s &= T - T_hg \\ \\ g &= aHT - agHT_h \\ \\ \dfrac{g}{T} &= \frac{aH}{1+T_hHa} \end{cases} \tag{3.1}$$

Where T_s is the search time, and T is the total time searching since last encounter. We may scale T to one, or view it as Δt which would be done in the case of differential equation. The Type II was originally derived experimentally by C.S. Holling by having blindfolded subjects forage in a room for discs. Of the three response types it is the only one which can be derived from first principles. Unless we consider handling to really be zero, in which case Type I and II would be equivalent.

The best way to understand Type III, is to graphically consider the shapes of the curves as in Figure 3.1. The Type II response is concave down, indicating the grazing rate of the predator is bounded. If we let the handling time tend to zero, however, we have the Type I response function, which is linear, or the grazing rate increase proportional to the population size of the prey. The Type III is not derived from first principles, however, the response has a sigmoid shape. This is to indicate a bounded grazing rate, due to handling time, as in the Type II. However the bottom of the

curve is accelerating with respect to prey population size. This acceleration is often used to model a system where the predator is switching its food preference.

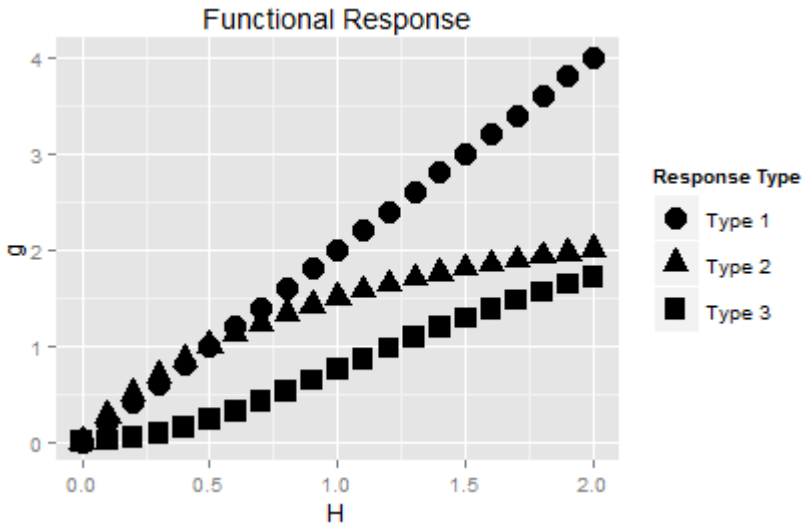

Figure 3.1: Graphs of Functional Response Types

3.2 LOTKA VOLTERRA AND SEIR

The research for this project involves modifying the continuous predator prey ecological model know as the Lotka-Volterra model, and the epidemic model know as the SEIR model, by adding a "kick" to the system. This kick, can be thought of as introducing a discrete event into an otherwise continuous system. First, however, we will consider continuous systems where there is no kick.

3.2.1 Lotka Volterra

The basic Lotka Volterra model is a differential equation model which considers a prey population with exponential growth in the absence of a predator, and a predator population which experiences an exponential decease in population size, or death, in the absence of prey. Linking the two populations is a functional response which effectively describes the rate at which prey are consumed and converted into new

predators. The model is described by equation (3.5) below [23].

$$\begin{cases} \dfrac{dH}{dt} &= rH - Pg(H,t) \\ \\ \dfrac{dP}{dt} &= wPg(H,t) - zP \end{cases} \tag{3.2}$$

- Functional Response: $g : C^2(\mathbb{R}) \times \mathbb{R} \to \mathbb{R}$
- Prey Population H
- Predator Population P
- Prey Growth Rate r
- Predator Death Rate z
- Efficiency of converting prey into predators w

It can be noted, as mentioned above, that rH indicates exponential growth in the absence of a predator since for $P = 0$, we have

$$\begin{cases} \dfrac{dH}{dt} &= rH \end{cases} \tag{3.3}$$

which a has solution at time t given by

$$\begin{cases} H(t) &= H(0)e^{rt} \end{cases} \tag{3.4}$$

Similarly, for $H = 0$ the term zP indicates exponential death for the predator. The functional response g is generally one of types I,II or III as indicated in Section 3.1.

3.2.2 SEIR

The SEIR model where S is for suspeticables, E is for latent, I is for infected, and R is for recovered and its variations are the basic ODE model for describing the

transmission of a disease through a population. It is similar in form to the Lotka Volterra model if we consider the group I to act like a predator. Below is a description of the standard SEIR model.

$$\begin{cases} \frac{dS}{dt} &= \mu - (\beta I + \mu)S \\ \frac{dE}{dt} &= \beta SI - (\mu + \sigma)E \\ \frac{dI}{dt} &= \sigma E - (\mu + \gamma)I \\ \frac{dR}{dt} &= \gamma I - \mu R \end{cases} \tag{3.5}$$

- Birth Rate μ
- Average Rate of Infection β
- Average Latency Period $1/\sigma$
- Recovery Rate γ

For the first equation dS/dt we have a constant birthrate μ. The term is constant since each class S, I, E and R are able to reproduce into the class S (disease transmission is not vertical to subsequent generations) and $S + E + I + R = 1$. Note that looking over each equation we have the terms $-\mu S, -\mu I, -\mu E$ and $-\mu R$ which sum to $-\mu$ or put another way, birthrate is equal to death rate. The term BIS appears in the equations for dS/dt and dE/dt. This is the rate of infection an can also be thought of as a Type 1 functional response $Ig(S)$, where infecteds are preying on susceptibles. It is assumed that before entering an infected state that these indivuals who contracted the disease will have a latent period where they do not have symptoms and cannot spread the disease. The rate at which individuals leave this class and become infected is σ, where $1/\sigma$ is the average latency period. Once an individual is infected they may

recover at a rate γ which also explains the last equation dR/dt. Note that there is no movement of individuals fomr the recovered class into the suseptiables class. This translates as individuals having life long immunity.

CHAPTER 4

A CASE STUDY ON CORAL REEF COMPETITION

Understanding reef dynamics provides a difficult challenge both experimentally and ethically. Consequently, in 2007 Mumby et. al. proposed a computer simulation, which was found to be faithful to time series data for Caribbean coral reefs, and an analytical model to help understand the dynamics of the simulation. The analytical model is a system of ordinary differential equations (ODE) and the authors claim this model demonstrates the existence of alternative stable states. Their existence, however needs further investigation. Namely, the existence of an alternative stable state should consider a sudden shift in coral and macroalgae populations (from a hurricane for instance) while the grazing rate remains constant. The results of such shifts, however, are often confounded by changes in grazing rate. Furthermore we might consider a system which exhibits alternative stable states in the absence of hurricanes may no longer do so in the presence of hurricanes with high frequency. Although the ODE does suggest alternative stable states, the ODE needs modification to explicitly account for discrete events such as hurricanes as previously mentioned. The goal of this study will be to investigate the simulation dynamics through a simplified analytical representation. We proceed by modifying the analytical model from Mumby et. al. by incorporating discrete changes into the ODE. We then analyze the resulting dynamics and their bifurcations with respect to changes in grazing rate and hurricane frequency. In particular a kick enabling the ODE to consider impulse events is added. Beyond adding a "kick" we employ the grazing function that is suggested by the simulation. The extended model was fit to the simulation data to support its use and predicts cyclic behavior depending nonlinearly on grazing rates

and hurricane frequency. The cycles may be thought of as alternative stable states in some cases, however, the existence of cycles adds new insight into consideration for reef health, restoration and dynamics.

4.1 INTRODUCTION

Coral reefs play an integral role in sustaining the world's biodiversity. This biodiversity provides aesthetic and commercial value with an emphasis on fisheries and tourism [12]. It is therefore easy to see how the livelihoods of millions of people that live in tropical coastal regions depend on healthy reefs [11, 22].

Reef health is typically characterized by the relative cover of macroalgae as well as coral [22]. Given the importance of reef health, however, we must ask if this simple characterization is enough. For instance, should we expect a healthy reef to have relatively constant characteristics over time or should we expect more complex dynamics? Some researchers have suggested that macroalgae- and coral-dominance are alternative stable states for reefs [16, 21]. Under this hypothesis, the fate of a reef is not completely determined by parameters such as grazing rate, but by the amount of macroalgae and coral present at a particular point in time. Large perturbations such as hurricanes could then move a reef between states, even if all other processes (growth, competition, grazing, etc.) remain unchanged.

For example, grazing by fish and urchins may be able to maintain a low level of macroalgae cover, despite the potential for macroalgae to overgrow coral. If the system is perturbed such that algal cover surpasses a critical level, this can overwhelm the ability of grazers to maintain the coral-dominated state [4, 21, 29, 20, 31, 33, 32]. This is thought to have occurred on the reefs surrounding Carrie Bow Caye in Belize. These reefs are in general remote and not heavily fished. Nevertheless, between 1980 and 1992 they transitioned from less than 5% macroalgae cover to over 60% macroalgae cover [33]. One possible explanation for this event is that a disease

caused a decrease in the coral population, allowing macroalgae the opportunity to take control of the reef. Despite the fact that parameters such as grazing rate had not changed, the coral was not able to recover from this event [33].

The existence of alternative stable states and cycles will be investigated through a case study of the Jamaican coral reefs from 1950-1984. However, with effects of global warming, and anthropogenic activity it may not be sufficient to study what happens when parameters remain constant. From 1950-1970 the Jamaican reefs had high densities of the sea urchin *Diadema antillarum* [12]. The large population of this echinoid species can likely be attributed to the substantial drop in fish biomass due to over-fishing, as the major predators and competitors of *D. antillarum* are fish [13, 12]. However, in 1982 and 1984 *D. antillarum* suffered population decreases as high as 99% [19, 12]. The loss of *D. antillarum* in addition to fish grazers, particularly parrotfish, is of considerable concern because the remaining grazers were not sufficient to restrain the growth of macroalgae and maintain reef health [16, 18]. What we see here is coral decline following a change in grazing rate [22]. In 1980 (two years prior to the decline in urchin density), Hurricane Allen severely damaged the Jamaican reefs [12]. Following the impact of the hurricane there was a short macroalgae bloom. Nevertheless, the corals began recovery shortly after possibly indicating a cyclic dynamic. By contrast, Hurricane Gilbert hit the Jamaican reef in 1988, and corals have not recovered even to this day [12, 14]. Separating these two events was the mass mortality of *D. antillarum*; hence, some biologists believe that the decline of this echinoid species changed the reef into a system with two alternative equilibrium points [16]. This may be true, however as previously stated, the coral decline began before Hurricane Gilbert, thus the change in grazing rate may confound the effect that Gilbert had on the reef. Also as previously noted, there is a period of coral recovery following Allen so it is natural to ask if the reef had more time to recover before that change in grazing rate or Gilbert, would the fate of the reef have been different? More

generally the interaction between grazing rate and hurricane frequency needs to be investigated when considering reef dynamics.

Using experimental manipulations to understand reef dynamics and the impact of hurricanes is generally logistically and ethically impossible. Hence, in 2007 Mumby et al. proposed a computer simulation, which was found to be faithful to time series data for Caribbean coral reefs. Mumby et al. simultaneously proposed a simplified analytical representation of the simulation, which allows for more formal mathematical description of the dynamics, including alternative stable states. However, the proposed analytical model is an ordinary differential equation (ODE) and does not explicitly account for the existence of hurricanes which are an integral part of reef dynamics [12].

The goal will be to investigate the reef simulation dynamics by extending the analytical representation from Mumby et al. to incorporate impulse events such as hurricanes. We aim to achieve this with two modifications of the model from [22]. First we insert an alternative grazing function that is consistent with the simulation model. Second we introduce a periodic kick into the system to account for the occurrence of hurricanes. This allows us to study non-stationary dynamics, with potentially important implications such as alternative stable states (which are typically modeled as point equilibria). The model will be shown to fit the data from the simulation, making it a viable candidate for studying reef dynamics. The modified model agrees with the findings of Mumby et al. that alternative stable states are possible. However, the new model indicates that these stable states are cycles and allows predictions for their existence and stability based on grazing rate and hurricane frequency. It should be noted that this is not the first attempt to study coral reefs by introducing discrete events into an otherwise continuous system [5]. What we add here however is to add discontinuities through a distribution along with a study of the resulting dynamics and their stability which could not be accomplished in [5]. We further review the the-

ory needed to understand the results. This addition is necessary for understanding dynamics such as alternative stable states and other dynamics which may be affected by impulse events such as hurricanes.

4.2 MODELS

We first present a brief description of the simulation model developed by Mumby et al. [22], as well as their ODE model, and we summarize their predictions. Next, we make the case that the grazing function in the ODE model should be modified to be consistent with the computer simulation. Then we add an explicit representation of hurricanes to the ODE model by incorporating sudden changes (kicks) to the state variables. In the following sections, we assess the fit of the new analytical model to the output of the Mumby et al. simulation model, and the resulting dynamics.

4.2.1 Revisiting the Mumby et al. Models

The simulation is a stochastic model presented as a square lattice of 2500 cells each approximating $0.25m^2$ of reef and occupied by algae, coral and ungrazable substrate. This model was designed to represent mid-depth (6-20 m) forereefs which typically harbor the highest biomass and diversity of reef organisms. Cover of each cell was updated in six-month time steps. Changes in coral cover were simulated using rates of recruitment and growth over algal turf, reproduction, and mortality. Macroalgae was supposed to grow vegetatively over both corals and algal turf. Grazing replaces both macroalgae and coral by algal turf; however, effects of grazing on coral are minimal. Competitive interactions between corals and macroalgae reduce each other's growth rates and are the only processes which occur across cell boundaries. Disturbance from hurricanes may occur at fixed times or as a Poisson process. In [22] Mumby et al simulated hurricanes at two distinct times representing hurricanes Allen in 1980 and Gilbert in 1988. The effect of the disturbance is to reduce macroalgae cover by 10%;

however the effects on coral are stochastic (see [22] for more details).

In the presence of urchins keeping a reef area of 42% in a grazed state every six months(or at the end of each discrete 6 month time step in the simulation 42% of the reef is free of macroalgae), the only stable state suggested by the simulation was coral dominated. However, in the event of urchin mortality, grazing becomes dominated by parrotfish which are able to keep from 5 to 40% of the reef in a grazed state during a six month period. Grazing in this range allows for two alternative stable states in the simulation, corresponding to dominance by either coral or macroalgae.

The ODE model consists of three variables, C, T and M representing the fraction of seabed covered by coral, turf algae, and macroalgae respectively. Specifically, this model uses the following system of ODE's:

$$\begin{cases} \dfrac{dM}{dt} &= aMC - \dfrac{gM}{M+T} + \gamma MT \\ \\ \dfrac{dC}{dt} &= rTC - \zeta C - aMC \end{cases} \tag{4.1}$$

where g, a, ζ, r, and γ represent the grazing rate, the rate macroalgae overgrows coral, the coral mortality rate, the rate coral overgrows turf, and the rate macroalgae overgrows turf respectively. Furthermore, algal turf is lost when overgrown by either coral or macroalgae and grows when coral dies or macroalgae is grazed. This results in the expression

$$\frac{dT}{dt} = \frac{gM}{M+T} + \zeta C - \gamma MT - rTC \tag{4.2}$$

which gives the condition that $d(M+C+T)/dt = 0$. Hence, if initial conditions $M(0), C(0)$, and $T(0)$ are chosen such that $M(0)+C(0)+T(0) = 1$ then the constraint that $M + C + T = 1$ holds for all time, and the model can be represented by (4.1) using this constraint. However, it still needs to be verified that $M + C \leq 1$, since we have to account for the case that T could be negative, in which case $M + C > 1$. Demonstrating that T cannot be negative amounts to considering the case where $T = 0$ in (4.2). This gives $dT/dt = g + \zeta C$ with $M \neq 0$. Next note that M and C are

never negative given positive initial conditions $M(0)$ and $C(0)$ since $dC/dt = 0$ when $C = 0$, and $dM/dt = 0$ when $M = 0$. Then for T to be non-negative it is sufficient that g and ζ are both non-negative or that $g \geq |\zeta|$. Observe, however, that all the parameters must be non-negative to have biological meaning. Then it follows that $dT/dt \geq 0$ when $T = 0$ and $M \neq 0$. Hence, if $T = 0$ the only possibility is that T stays 0 or increases. Consequently T is never negative and $M + C \leq 1$.

Mumby et. al [22] claim the following dynamics are present in the ODE model.

- **Only** a macroalgae dominated stable state, with low coral cover.
- **Both** a coral dominated stable state,with low macroalgae cover, and a macroalgae dominated stable state with low coral cover, indicating two alternative stable states.

However not presented in [22] the dynamic of only a coral dominated stable state, with low macroalgae cover is implied by the model.

Unlike the computer simulation, however, the ODE model does not account for the occurrence of hurricanes, which are highly integrated with reef dynamics [12].

4.2.2 Modification of the Grazing Function

Another distinction between the ODE model (4.1) and the simulation is that the ODE model uses the grazing function $gM/(M + T)$, which is inconsistent with the rules that specify grazing in the simulation model. In the simulation reef cells($0.25m^2$ of reef area) are grazed at random until a certain percent of the reef has been grazed [22]. Biologically if we were to consider a handling time in the process this would suggest using the Holling Disc equation as the response function, or gM when the handling time is negligible or not considered at all as in the simulation. This equates to the parrotfish keeping 40% of the reef area clear of macroalgae in each 6 month time step which is how grazing is measured in the simulation. We implement this by

selecting 40% of cells at random in each time step, and any of the selected cells that contain macroalgae are converted to turf. In order to translate this grazing rate to a continuous time model, we require a grazing function $G(M, T)$ such that the solution to

$$\frac{dM}{dt} = -G(M, T) \tag{4.3}$$

is $M(t) = 0.6M(0)$ at $t = 6$ months, regardless of the initial value $M(0)$. Under the assumption that grazers clear cells at random, the fraction of macroalgae converted to turf should also be independent of the values of $T(0)$ and $C(0)$, i.e., $G(M, T) = G(M)$ depends only on the fraction of cells occupied by macroalgae.

For example, suppose the grid contains 100 cells, and initially 30 contain macroalgae, 30 contain turf, and 40 contain coral, i.e., $M(0) = 0.3$, $T(0) = 0.3$, and $C(0) = 0.4$. Under the assumptions described above, $0.4 \times 30 = 12$ macroalgae cells will be converted to turf. Alternatively, suppose 30 contain macroalgae but 50 contain turf. The assumption that grazers select cells at random implies that 12 macroalgae cells will be converted to turf in this case as well. However, $M/(M + T)$ differs between the two cases, which implies that the grazing function $gM/(M + T)$ in the ODE is inconsistent with the assumptions that define the simulation model.

The simplest grazing function that satisfies this property is $G(M, T) = gM(t)$, and we show that this function provides a better fit to the simulation model in Section 3.4. The solution to the differential equation (4.3) above, $M(t) = M(0)e^{-gt}$ with $M(t)/M(0) = 0.6$ suggests that $g = -\log 0.6$. Hence, a further problem arises with the parameterization of the ODE model in Mumby et al. (2007), who assumed $g = 0.4$, i.e., the grazing rate in the continuous time model is equal to the fraction of cells grazed in each 6 month time step in the discrete time simulation model. For example, if we rescaled time from 6 month time steps to 3 month time steps, the value of g and other parameters would have to be adjusted accordingly. For an ODE we let the time step decrease to 0, so change is instantaneous and we must rescale

parameters just as we must rescale for the 3 month time step.

Replacing $gM/(M+T)$ by gM in (4.1) yields the following model:

$$\begin{cases} \dfrac{dM}{dt} &= aMC - gM + \gamma MT \\ \\ \dfrac{dC}{dt} &= rTC - \zeta C - aMC \end{cases} \tag{4.4}$$

Note that, as in the previous section, it is also true for this system that $M+C+T=1$ if the initial conditions sum to 1, and that $M+C \leq 1$ if g, ζ are both non-negative. Using the constraint that $M+C+T=1$ we can rewrite (4.4) as

$$\begin{cases} \dfrac{dM}{dt} &= (a-\gamma)MC + (\gamma - g)M - \gamma M^2 \\ \\ \dfrac{dC}{dt} &= (r-\zeta)C - (a+r)MC - rC^2 \end{cases} \tag{4.5}$$

Evaluating the model requires values for the model parameters. Because Mumby et al. (2007) do not provide values for the ODE model parameters other than g, and in light of the problem noted in the previous paragraph of translating discrete into continuous parameters, we took the approach of fitting the parameters to simulation model output as described below in Section 3.4.

4.2.3 Adding Discrete Kicks to an ODE

We incorporate an explicit representation of hurricanes into the ODE model as discrete changes, or kicks, in the dynamics of coral, macroalgae, and turf. A kick is added to the system through the Dirac distribution δ, defined in the Preliminaries-Mathematics section of the introduction.

Addition of kick terms to (4.4) results in

$$\begin{cases} \dfrac{dM}{dt} &= aMC - gM + \gamma MT + \sum_{n=0}^{\infty} h_1(1-M)\delta(t-nk) \\ \\ \dfrac{dC}{dt} &= rTC - \zeta C - aMC + \sum_{n=0}^{\infty} h_2 C\delta(t-nk) \end{cases} \tag{4.6}$$

where h_1 and h_2 are constants and $k > 0$ is the period at which hurricanes occur. The index $n \in \mathbb{N}$ can be equated to the number of six month time steps which have occurred in the corresponding simulation model. At the time of the n^{th} kick, $t = nk$ and the integral of $\delta(t - nk)$ is nonzero which causes a discrete change in both M and C, thus mimicking the drastic changes in dynamics that we would expect in the event of a hurricane. In dC/dt the Dirac distribution is multiplied by $h_2 C$ with $h_2 < 0$, which represents loss of coral during a hurricane, as in the simulation model. Similarly, in dM/dt the Dirac distribution is multiplied by $h_1(1 - M)$ with $h_1 > 0$ to represent the increase in macroalgae immediately following a hurricane, also consistent with the simulation model assumptions. This increase can only occur on the fraction of the reef that is not already occupied by macroalgae.

We show how the kick is integrated and that (4.6) predicts the amount of macroalage and coral will be after a kick occurs. These predictions are then matched against simulation data in Section 3.4 which support our choice of kick. Let c_a represent the amount of coral just after the m^{th} kick and let c_b represent the amount of coral just before the m^{th} kick. Then using (4.6) we may divide both sides of the expression by C and integrate to obtain

$$\int_{c_b}^{c_a} \frac{dC}{C} = \int_{mk-\epsilon}^{mk+\epsilon} (rT - \zeta - aM + \sum_{n=0}^{\infty} h_2 \delta(t - nk))dt, \tag{4.7}$$

or equivalently we may write

$$\int_{c_b}^{c_a} \frac{dC}{C} = \int_{mk-\epsilon}^{mk+\epsilon} (rT - \zeta - aM)dt + \int_{mk-\varepsilon}^{mk+\varepsilon} \sum_{n=0}^{\infty} h_2 \delta(t - nk)dt. \tag{4.8}$$

Because $(rT - \zeta - aM)$ is bounded, we have

$$\lim_{\epsilon \to 0} \int_{mk-\epsilon}^{mk+\varepsilon} (rT - \zeta - aM)dt = 0. \tag{4.9}$$

For $0 < \varepsilon < k$, the only non-zero term in the sum in (4.8) is when $m = n$. Hence,

$$\lim_{\varepsilon \to 0} \int_{c_b}^{c_a} \frac{dC}{C} = \lim_{\varepsilon \to 0} \int_{mk-\varepsilon}^{mk+\varepsilon} (rT - \zeta - aM)dt + \lim_{\varepsilon \to 0} \int_{mk-\varepsilon}^{mk+\varepsilon} h_2 \delta(t - nk)dt, \tag{4.10}$$

which by (4.9) becomes

$$\lim_{\varepsilon\to 0}\int_{c_b}^{c_a}\frac{dC}{C}=\lim_{\varepsilon\to 0}\int_{mk-\varepsilon}^{mk+\varepsilon}(h_2\delta(t-mk))dt. \tag{4.11}$$

Applying the definition of δ on the right and integrating as usual on the left we have

$$\lim_{\varepsilon\to 0}\log\left(\frac{c_a}{c_b}\right)=h_2. \tag{4.12}$$

Since there is no dependence on ε we may ignore the limits and write

$$c_a=c_b e^{h_2} \tag{4.13}$$

and by using a similar argument we write

$$m_a=1-\frac{1-m_b}{e^{h_1}}, \tag{4.14}$$

where m_a and m_b denote the amount of macroalgae in the reef immediately after and before the m^{th} kick, respectively. We define τ_a as the amount of turf present immediately after the m^{th} kick and τ_b as the amount of turf present immediately before the m^{th} kick, as well. For the system to stay conserved we require

$$c_a+m_a+\tau_a=1 \tag{4.15}$$

which implies

$$\tau_a=1-c_a-m_a=\frac{1-m_b}{e^{h_1}}-c_b e^{h_2}. \tag{4.16}$$

Now the requirement that $m_a+c_a\leq 1$ is the same as $\tau_a\geq 0$, which is equivalent to

$$e^{h_1+h_2}\leq 1. \tag{4.17}$$

Thus all we require for the condition $m_a+c_a\leq 1$ to hold is that $e^{h_1+h_2}\leq 1$ or, equivalently, $h_1\leq|h_2|$.

We have illustrated how to evaluate (4.6) in Fig. 4.1. The continuous part of (4.6) given by (4.4) is integrated until the time of the kick. Then (4.13) and (4.14) are applied to the corresponding state variables, followed by integrating (4.4) until the time of the next kick.

4.2.4 Kicked Cycles

A cycle for an ODE requires a time period $p > 0$ and an element of the state space, say x such that $\phi(x, p) = x$ but $\phi(x, t) \neq x$ if $t < p$, where ϕ is the flow for the ODE in question. The flow, however, is a dynamical system with the property that times are additive under composition of state variables. For instance using function composition, we have that if $\phi(x, t) = \phi_t(x)$ then $\phi_{p/2}(\phi_{p/2}(x)) = \phi_p(x) = x$. The dynamic of a cycle can then be looked at as a periodic point for a map through function composition. This is the how we will treat cycles, as fixed points of maps. Due to the nature of the kick we might expect any periodic motion to have a continuous part and a discrete part. Since this periodic motion can be treated as a fixed point of a map, standard stability analysis still applies. Refer to Section 4 for more details.

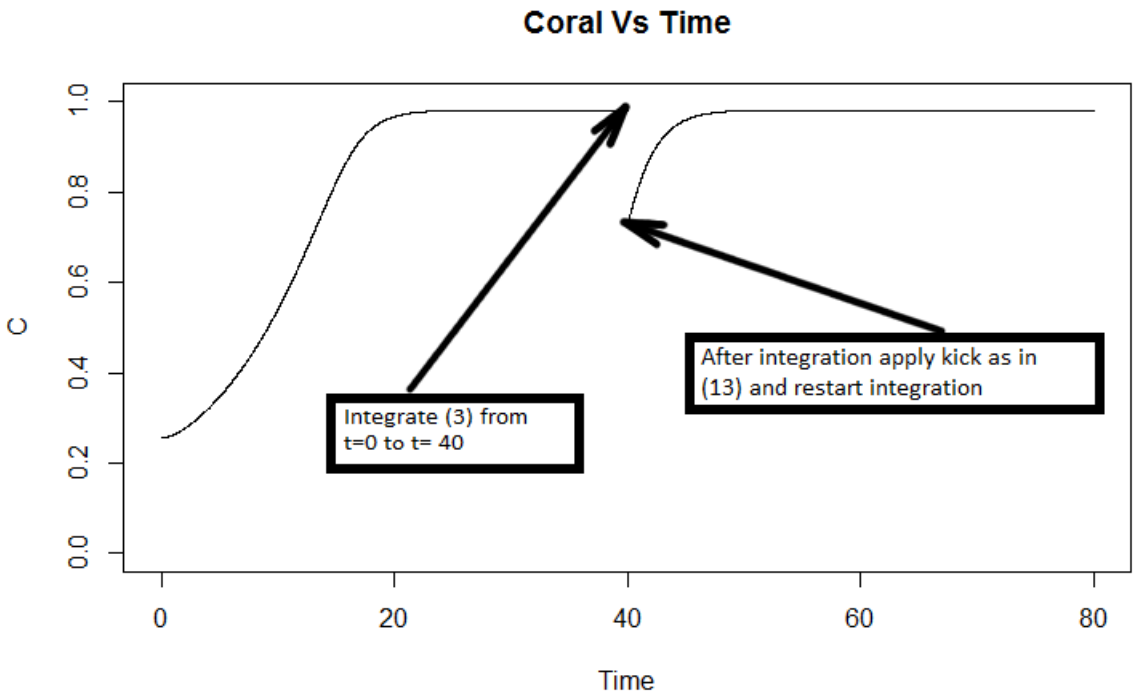

Figure 4.1: Demonstration for the numerical integration of (4.6). This is done by integrating (4.4) until the time of the kick, noting that (4.4) is equivalent to (4.6) with the kick removed. The kick is then applied using (4.13) for coral, or (4.14) for macroalgae. After the kick is applied, we start the procedure over by integrating (4.4).

4.3 SIMULATION EXPERIMENTS

Before proceeding with the analysis of the model in (4.6), we wish to determine how well the simplification captures the dynamics predicted by the simulation model. We first demonstrate that the grazing in the simulation is better fit by our modified grazing function than by the function in (4.1). Next, we use simulation output for hurricane disturbances to find values for the parameters h_1 and h_2, as suggested by equations (4.13) and (4.14). Note that R^2 values close to 1 would indicate that h_1 and h_2 should have the same values between trials. We then fit the full model in (4.6) to provide a more formal assessment of its overall ability to mimic the simulation model.

4.3.1 Simulation Parameters and Specifications

We ran 10 trials of the simulation model for 100 time steps each, representing 50 years. Each simulation included two disturbances, representing the impacts of hurricanes Allen and Gilbert on the Jamaican reefs. Mumby [21] used initial conditions of 10% macroalgae and 35% coral. We varied these initial conditions to obtain a broader range of the system dynamics (Table 4.1). We also varied the fraction of total area grazed per time step ("Parrotfish Grazing" in Table 4.1) to span the range over which different stable states arise. No other parameters varied between trials. However, we note three key differences between the simulation and the simplified representation in the differential equation model. First, the simulation model allows stochastic variation in cell transitions between states, whereas the differential equation model is deterministic. Second, the simulation model distinguishes populations of brooding and spawning coral species (with different demographic rates), which are lumped together in the differential equation model. Finally, the simulation model contains 10% ungrazable reef area, which is ignored in the differential equation model. Given these differences, we expect some variation in fit of the differential equation model

over different runs of the simulation.

Trial	Parrotfish Grazing	Brooders	Spawners	Ungrazable Reef Area	Macroalgae	Turf Algae
1	10	15	15	10	20	40
2	40	15	15	10	20	40
3	40	15	15	10	20	40
4	30	15	15	10	20	40
5	30	10	10	10	20	50
6	20	10	10	10	20	50
7	15	10	10	10	20	50
8	17.5	10	10	10	30	40
9	18	10	10	10	20	50
10	18	70	10	10	5	5

Table 4.1: The grazing rate and initial conditions for each trial of the simulation. Note that trials 2 and 3 were run identically to consider stochasticity. Turf is referred to as cropped algae in Mumby's presenstation of the simulation model [21].

4.3.2 Transitions from Macroalgae to Turf

During each 6 month time step in the simulation, the fraction of area which transitioned via grazing from macroalgae to cropped algae was recorded, along with the values of M and C. In order to assess the fit of the two grazing functions, we plotted the transitions against M and $M/(1-C)$, where the latter is equal to the grazing function in (4.1), i.e., $1 - C = M + T$. The data in the transition plots suggest that the grazing function should be gM and not $gM/(1-C)$.

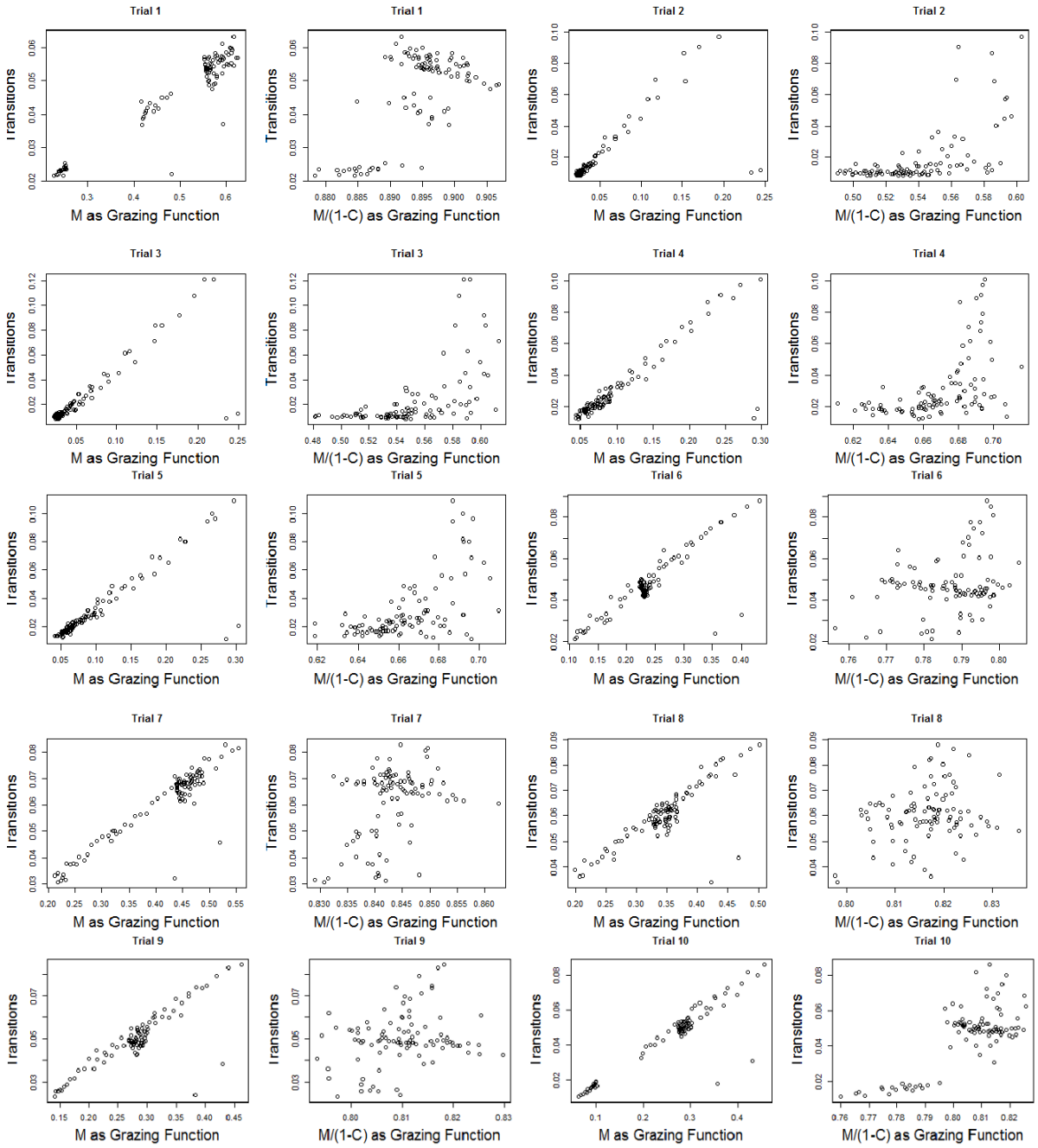

Figure 4.2: The fractions of area which transitioned from macroalgae to cropped algae versus M and $M/(1-C)$ for each trial, where M is the area of macroalgae present after grazing, and C is the area of coral present after grazing.

4.3.3 Kicks

Equation (4.13) predicts that the amount of coral present after a kick is proportional to the amount of coral present before a kick. Similarly, rearranging equation (4.14) predicts that one minus the amount of macroalgae present after a kick is proportional to one minus the amount of macroalgae present before a kick. If this model is correct, it makes sense to find h_1 and h_2 by linear regression, and R^2 (fraction of variation that the model can explain) values close to 1 would suggest that these parameters stay fixed. Since a total of ten simulations were completed, with two hurricanes each, we were left with 20 points immediately before and after each hurricane for both coral and macroalgae. These data are plotted in Figure 4.3 with corresponding linear regression lines. The regression line for macroalgae was forced to have an intercept of 0 to be consistent with (4.14), which does not have an intercept term.

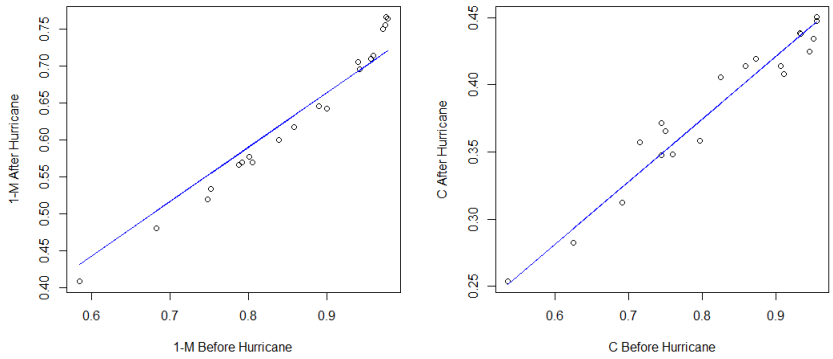

Figure 4.3: Left panel: $1 - M$ after a hurricane vs. $1 - M$ before a hurricane. Right panel: C after a hurricane vs. C before a hurricane. The slope of the lines was used to calculate h_1 and h_2 from equations (4.13) and (4.14). Note that the intercept for the line on the left was forced to be 0 for consistency with (4.14).

Based on the data presented in Figure 4.3, e^{h1} and e^{h_2} from equations (4.13) and (4.14) were estimated with R^2 values close to 1, as indicated in Table 4.2.

Coefficient	Coefficient Estimate	h Estimate	R^2	p-value
e^{h_1}	1.355554	0.3042104	0.998	$p \leq 2.2e-16$
e^{h_2}	0.4681111	-0.7590495	0.998	$p \leq 2.2e-16$

Table 4.2: Estimates of e^{h_1} and e^{h_2}, as the slopes of line on the left and on the right respectively in Figure 4.3. h_1 and h_2 are defined in (4.6).

4.3.4 Model Fitting

We used the software DDEFIT [34] to fit the ODE model (4.6), with h_1 and h_2 given in Table 4.2, and the output from the ten runs of the simulation. The resulting parameter values are listed in Table 4.3, and the fits are plotted with the corresponding simulation data in Figure 4.4. Both the simulation data and the ODE model from (4.6) seem to indicate the existence of three stable states which will be explored later through our model. Trials 1 and 7 through 10 indicate a macroalgae dominated stable state, trial 6 indicates a stable state dominated by both macroalgae and coral, while trials 2 through 5 indicate a coral dominated stable state. The coral dominated stable states are characterized by coral recovery after each hurricane resulting in a cycle rather than a fixed point. The existence of cycles is an important result, because the quality of the fits suggests moving beyond the notion of stable states that stay constant over time to include the study of cycles and their stability.

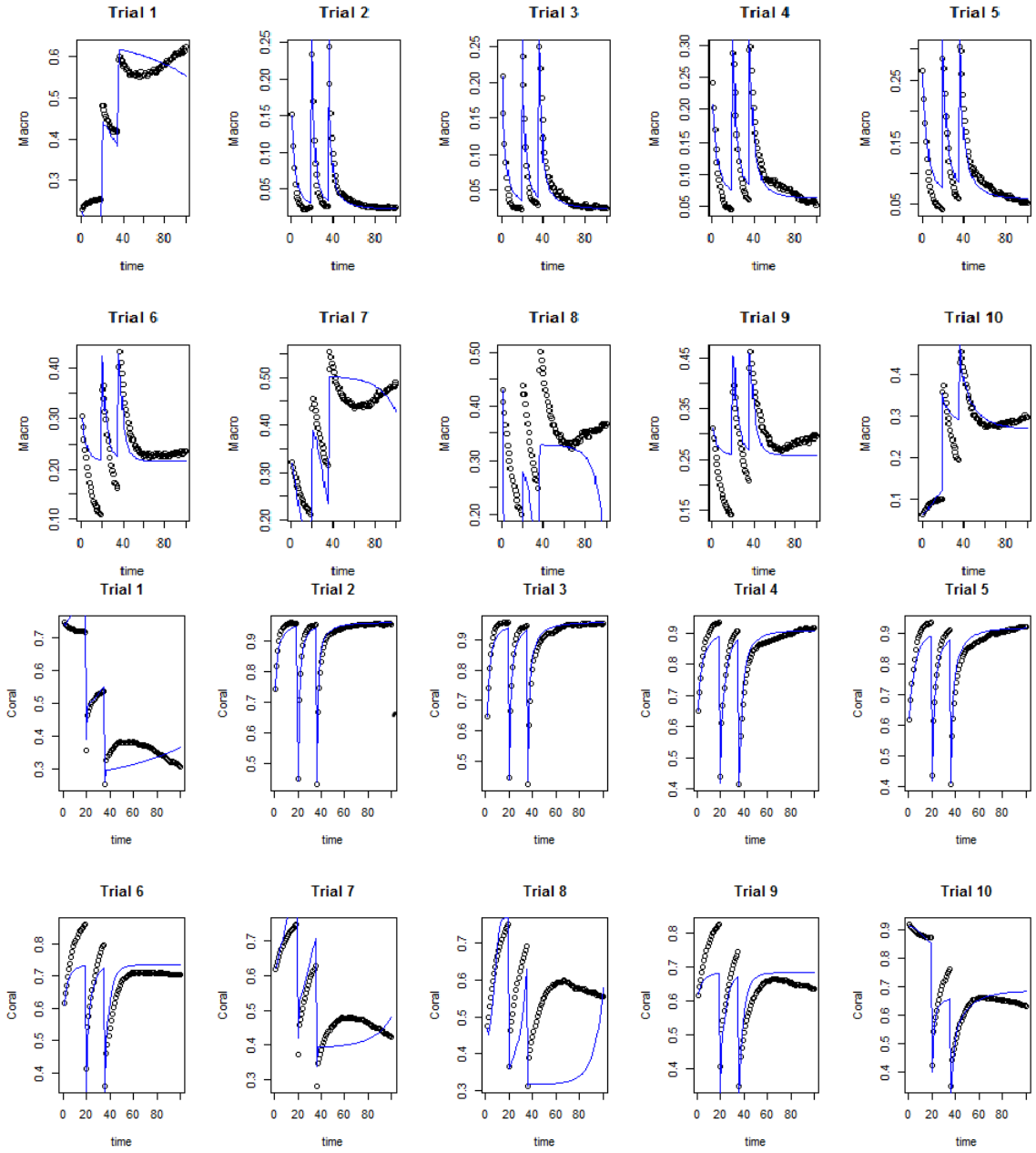

Figure 4.4: Time series of coral and macroalgae cover output by the ten simulation model runs (open points). Best fits of the ODE model (4.6) to each run are indicated by solid lines.

Analyses of the fits are included in Table 4.3. Trials 2-5 and 10 have R^2 values above 90% and Trial 1 has an R^2 value above 86%. Trials 6 and 9 capture the qualitative aspects of the simulation very well (Fig. 4.4), however the magnitudes of

the kicks are not sufficient as can be visually verified. This would likely be improved if we considered a density dependent kick where the magnitude of the "kick" depends on the state variables instead of being constants such as e^{h_2} (see section 5 for more details). However, the values of e^{h_1} and e^{h_2} were used as constants (Table 4.2) because of the strong linear correlation present in (4.3). For Trials 7 and 8, the parameter fitting algorithm converged to parameters such that the data passes very close to a saddle point for the ODE portion of the model. We should expect fitting to be difficult in this case, but this does not indicate a problem with the model.

Trial	a	g	γ	r	ζ	R^2
1	1.43132	2.13004	19.9529	17.5921	0.616125	0.865
2	3.29176	3.22782	3.81907	5.70696	0.0335	0.961
3	3.22956	3.18399	4.71234	5.65991	0.0375	0.951
4	2.68234	2.59592	5.37369	5.85168	0.00951	0.921
5	1.2731	1.20764	1.63061	3.32021	0.00894	0.91
6	1.97705	1.75323	6.07667	8.68713	0.00325	0.598
7	3.34462	3.89748	24.8945	19.6683	0.35752	0.601
8	0.406736	4.38121	12	1.07423	0.246807	NA
9	1.81292	1.70302	8.0787	12	0.219467	0.498
10	0.185241	0.126891	0	1.47786	0.0213	0.923

Table 4.3: Parameter values and R^2 for fits of the model in (4.6) to the ten simulation model runs.

4.4 DYNAMICS

The model given by the equations in (4.4) had four equilibrium points, three of which are given by

$$\{(0,0),((\gamma-g)/\gamma,0),(0,(r-\zeta)/r)\}, \tag{4.18}$$

where the first coordinate represents the fraction of macroalgae cover and the second coordinate represents the fraction of coral cover. The fourth critical point is given by the equations

$$M = -\frac{(\gamma-a)\zeta+(a-g)r}{a\gamma-ar-a^2}, \tag{4.19}$$

$$C = \frac{\gamma(\zeta+a)-g(r+a)}{a\gamma-ar-a^2}. \tag{4.20}$$

This equilibrium point can be an attractor or a saddle, depending on parameter values. The parameters in trial 6 result in an attractor for Eq. (4.19)-(4.20), with repellers on the positive M and C axes. Trial 8 parameters result in a saddle, with attractors on the positive M and C axes denoting an alternative stable state (see Figure 4.5).

However, we wish to investigate the dynamics of the modified model (4.6) with explicit representation of hurricanes, i.e., we ask how the addition of a kick affects the alternative stable states predicted with parameter values from trial 8. We chose to work with trial 8 because the parameters for the unkicked part of the system result in the existence of two alternative stable states similar to that suggested in [22]. We can then take this case and consider how changes in grazing rate and hurricane frequency interact to effect the dynamics of the full model. In other words we are addressing the question of whether a model which looks at reef dynamics through grazing rate is sufficient or whether grazing rate and hurricane frequency should be considered together when describing reef dynamics.

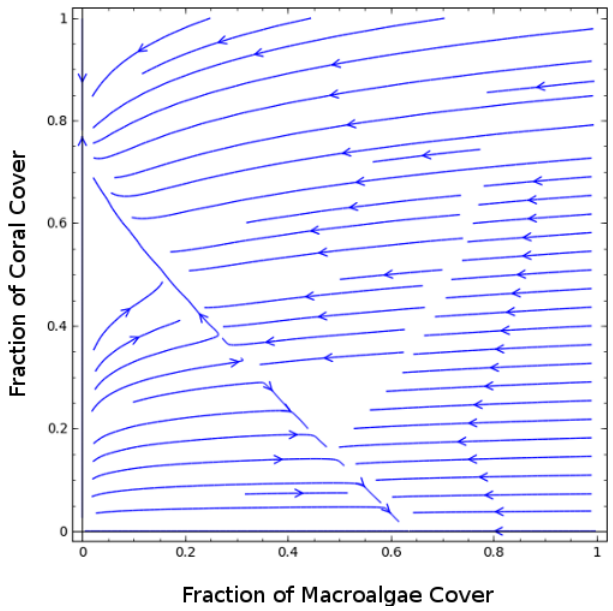

Figure 4.5: Phase plot for equations (4.5) using parameters from trial 8 in Table 4.3.

For the unkicked system, starting with initial conditions close to the attractor on the M axis, adding a kick will just move the system closer to the attractor on the M axis since the kick decreases the coral and the underlying vector field will eventually point toward the M axis (Fig. 4.5). It should be noted that the M axis is invariant and the macroalgae dominated state for the ODE may not be the same as for the kicked system. Consequently, we take initial conditions near the attractor on the C axis for the unkicked system to see if the initial conditions still converge to a coral dominated state. The data in Figure 4.6 are taken from the kicked system with the parameters from trial 8 and a hurricane occurring once every 20 years. The figure demonstrates that the stationary alternative stable state dominated by coral has evolved into fixed point for our kicked map but viewing the action continuously over time as a cyclic behavior.

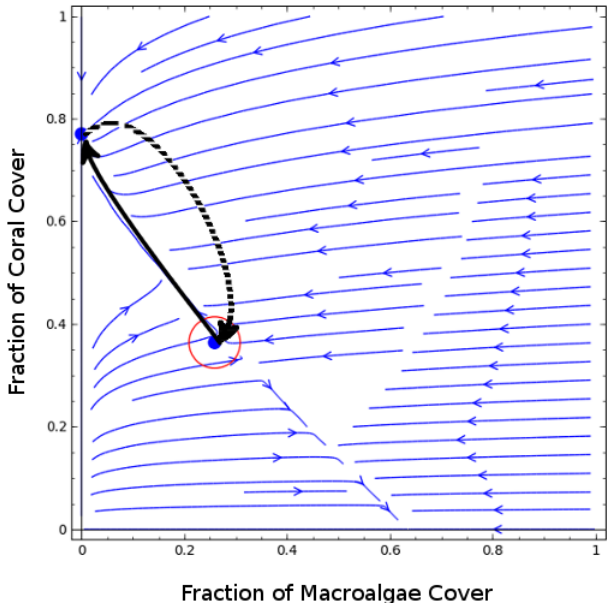

Figure 4.6: The phaseplot for the ODE given in (4.5) with parameters from trial 8 is displayed by the solid arrows. A kick occurring every 20 years was added, as in (4.6), and is indicated by the dashed arrow. This results in a cycle between the two filled in circles. The unfilled circle represents a region of perturbation for which the cycle is stable. Numerical results suggest that all points outside the unfilled circle closer to coral converge to this cycle.

For the same scenario presented in Figure 4.6, except with a kick occurring once every 10 years, the cycle no longer exists and the system converges to a macroalgae dominated state. Further investigation of this cycle is displayed in Figure 4.7. The analysis in Figure 4.7 was conducted by searching for fixed points, via a grid search and Newton's method. The fixed points considered for the flow where were neither M nor C were 0 for varying parameter ranges of g and K. Once a fixed point for the flow is found, we numerically calculated the eigenvalues for the flow. This is done by first integrating the underlying ODE to the kick time and applying the kick to create a numerical approximation for our map. Now we may apply the definition of the derivative to this map to estimate the partial derivatives of the Jacobian at the fixed point and the corresponding eigenvalues to determine stability. Since we are dealing with a map, eigenvalues with absolute value greater than 1 are unstable, less than 1

are stable and equal to 1 are not hyperbolic. It should be noted that the Jacobian for stability analysis and Newtons Methods were done in the same manner.

What Figure 4.7 illustrates is that a system which does not consider hurricane frequency and impact can be misleading. For instance the figure suggests it is possible to have a system where the unkicked model results in alternative stable states for a particular grazing rate, however the model including hurricane frequency does not. The unkicked model also indicates that researches should look for convergence to stationary states instead of studying cyclic trends for the reef, which we have argued is not correct.

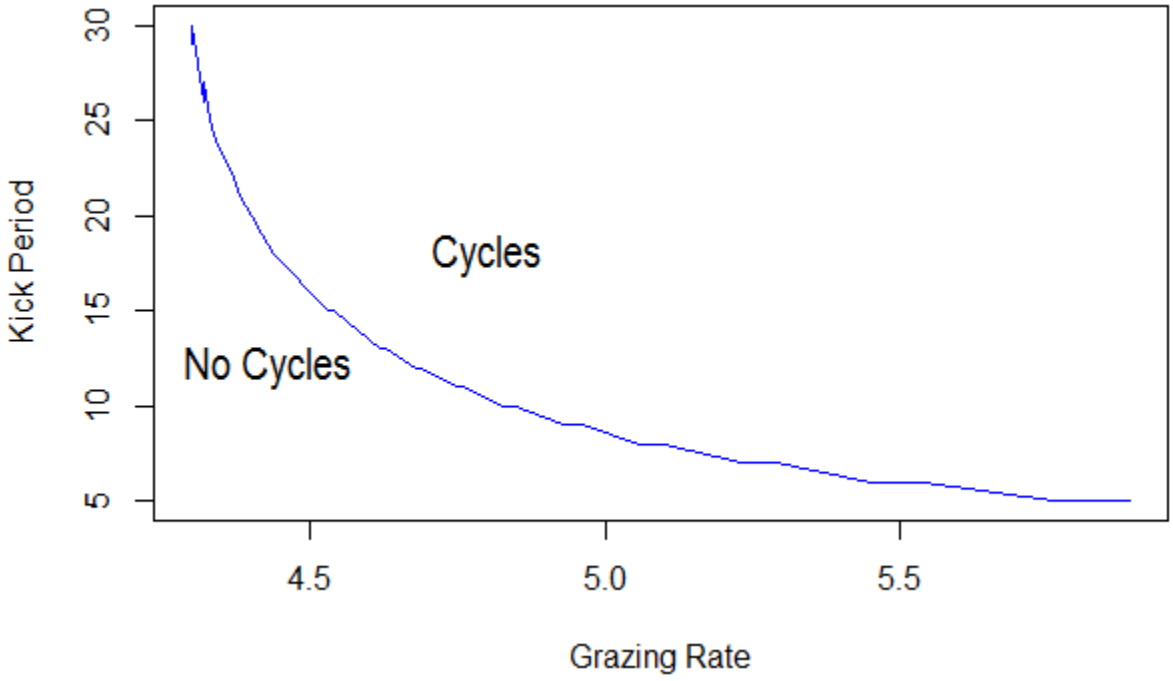

Figure 4.7: Stability analysis of the cycle displayed in Figure 4.6 for a range of values of grazing rate (g) and time between hurricanes (K). All other parameters are from Trial 8. The blue line represents pairs (g, K) for which the cycle is unstable. Pairs above and to the right of the blue line are consistent with stable cycles. No cycles were detected for points below and to the left of the blue line.

4.5 DISCUSSION

This study aims to investigate the dynamics of coral reefs by studying an analytical representation of a computer simulation found to be faithful to reef dynamics. Understanding these dynamics is becoming increasingly important due to the livelihoods of millions of people world wide depending on these habitats. Processes such as global warming and anthropogenic effects make the study of impulses and how reef dynamics depend on parameters such as hurricane frequency and grazing rate a necessity. The investigation proceeded by modifying the model from Mumby et al. [22] in two ways. First, we offered an alternative for the grazing function that is consistent with the simulation, as shown in Figure 4.2. In particular, a grazing function given by gM was used in place of $gM/(1-C)$. The reason for this choice is that the simulation results in Figure 4.2 indicate that macroalgae is grazed at a rate proportional to the amount of macroalgae in the reef. Having the correct grazing function allows us to better understand the dynamics of the simulation. The second modification to the model was to introduce a periodic "kick" into the system to simulate the occurrence of hurricanes. The model with the new grazing function and kicks is given in (4.6), requiring values for h_1 and h_2 with $h_1 \leq |h_2|$ as discussed in the experiment section and given in Table 4.2.

The simulation from Mumby et al. has been shown to faithfully emulate reef dynamics [22]. To show our modified model is faithful to the simulation, we recoded the simulation and fit the model results to the simulation data. Note that all the fitted parameters are positive (see Table 4.3) which is sufficient to guarantee that $M + C \leq 1$, resulting in a closed system.

The simulation data (Figure 4.4) were fit reasonably well with 5 of the trials having R^2 values above 0.9 (see Table 4.3) and all but trials $1, 7, 8, 9$ capturing the qualitative information. The loss of this information was not due to the inability of the model to emulate these features, as can be seen by inspecting the time series plots for trials

$2, 3, 4, 5, 6$ and 10 in Figure 4.4. One way to improve these fits however, maybe to add density dependence to the kick terms so h_1 and h_2 would depend on the amount of coral and macroalgae in the reef. This would also be more consistent with the simulation design.

The parameters selected by DDEFIT, for Trial 8, reveal a saddle point at $M \approx C \approx 0.32$. Since the data in trial 8 (see Figure 4.4) pass close to this point, we should expect some numerical instability. This, however, does not necessarily indicate a problem with the model, only the fitting method. A similar problem occurred with Trial 7. Based on the results of the fitting we considered the model to faithfully describe the dynamics of the simulation. This result provides justification for using our analytical model for studying the simulation dynamics.

As mentioned in the results section, trial 8 fitted parameters indicate the existence of alternative stable states for the model without a kick (see Figure 4.5). In this case, for the unkicked system if we chose a point sufficiently close to the attractor on the M axis then the kick, moving in the same direction as the flow, would not change the fate of the system as macroalgae dominated. Thus we are interested in the behavior of points that lie near the attractor on the C axis. A kick here would be opposed to the direction of the flow making it unclear if the addition of a kick still allows for two alternative stable states.

Looking at Figure 4.6, we notice that two alternative stable states are possible, although one of the alternative stable states predicted is a cycle. This is an important point as it changes the types of dynamics we should study when considering the behavior of coral reefs. It should be noted however, that this cycle depends nonlinearly on both grazing rate and hurricane frequency as can be seen in Figure 4.7. This nonlinear interaction suggests that the change in grazing rate after hurricane Allen may confound the effect that Gilbert had on the reefs. For instance, coral was already declining when Gilbert hit, so the impact may have just sped up what was already

happening. Also suppose there were no change in grazing rate, then the effect of Gilbert may have just been to continue a cyclic pattern. Without an appropriate model or data, which we currently do not have, it would be impossible to make this distinction. It would be interesting to fit either the actual data from the Jamaican Reef or data from the simulation with the same parameters used in [22]. We then could consider a bifurcation diagram as in Figure 4.7 and make predictions about the effect of a hurricane, such as Gilbert, with or without changes in grazing rate.

A possible concern is that hurricanes occur stochastically and not with a constant frequency. One response to this would be to interpret the hurricane frequency as the expected value of a Poisson distribution. One could then, using Figure 4.7, calculate the probability that the cycle becomes unstable or vanishes. Another approach as used in [5] is to use a Poisson jump process. This of course introduces other complications with stability analysis and may be a direction for future study. The appearance of cycles is important, because it presents a paradigm shift in how we think about coral reef health. Instead of considering the health of a reef based on coral and macroalgae concentrations at a particular point in time, it becomes appropriate to look at stable patterns that vary over time instead.

A further benefit that may result from studying the effect of impulse dynamics on reefs is because unlike the ODE model presented, hurricanes destroy both coral and macroalgae. Thus hurricanes could be used as a means of reef restoration [8]. Consequently, the current mathematical models should be made more flexible to consider kicks that allow for increases in coral under the relevant circumstances. Further interest may be to consider the dynamics of the reef with respect to coral age. For instance, the effect of a hurricane may be dramatically different for a reef dominated by juvenile coral as opposed to one covered by mature corals as in the computer simulation.

CHAPTER 5
CASE STUDY FOX RABIES

5.1 INTRODUCTION

Rabies remains an important human health and wildlife management concern worldwide. The presence of rabies in an area exacerbates the uncertainty of conserving rare and threatened mammals[30].The disease is transmitted through the saliva of infected animals and affects the central nervous system. All mammals are thought to be susceptible to this disease and throughout human history it has been one of the most feared of all infectious diseases [3].

Currently underreporting of human deaths from rabies in many parts of the world is significant [1]. For instance, concerning Fox Rabies in Europe the proportion of all cases that are observed is likely to be as low as two to ten percent [10]. In order to address problems such as properly estimating the impact of the disease and eliminating it all together, The World Health Organization's(WHO) Expert Advisory Panel on Rabies has partnered with entities such as the Bill and Melinda Gates Foundation, the Global Alliance for Rabies Control and the Partnership for Rabies Prevention. Those joint efforts have begun to break the cycle of rabies neglect, and rabies is becoming recognized as a priority for investment [1]. Consequently, methods have been developed to estimate the mortality attributable to rabies. In particular predictive models have been investigated [1]. When rabies penetrates a new area, there is a peak in reported cases among foxes.

Modeling offers a relatively inexpensive, way to examine what factors affect rabies transmission as well as management and economics [30]. For instance modeling

techniques have resulted in a revised estimate of the burden of rabies in Africa and Asia. [1].

The modeling of rabies in general involves many complex interactions which depend on both space and time dependent aspects. For instance, concerning fox rabies, dispersal and competition for fox territories results in increased chances of encounters in late winter. Also vixen tend to peak in their number of interactions during the summer due to the physiological strain of reproduction. Migration of juvenile foxes, usually in the fall, tends to influence regions of low population density since dispersal distances tend to correlate negatively with population density [10]. If we consider the effects of these dependencies we note the observation of interesting dynamics. For instance epidemic cycles of increasing amplitude [3], and in Russia, there are different rabies cycles in foxes and dogs in the same area at the same time [10].

A novel attempt in modeling fox rabies was made in a paper by Anderson et al [3]. This paper attempted to model fox rabies in Europe by using a system of ordinary differential equations (ODE's) where most prior models were computer simulations and statistical models. The model makes an additional contribution by allowing population size to be dynamic. Here we wish to make an additional contribution. As noted there are times during the year where contact rates are higher, such as when juvenile foxes disperse, or when a neighboring community practices rabies control via culling thereby disrupting the fox's social structure [3]. Consequently, over a very small time period there may be an increase in the number of infected individuals of a population.

5.2 MIGRATION

The details of the model in [3] will be explored later on, however, what Anderson et al., while noting its importance, do not consider in their model, is migration.

Wildlife rabies emerged in Europe after dog rabies was eliminated, the new pri-

mary host being the red fox (*V. vulpes*). Coming from the east, fox rabies spread inexorably across the continent within a few decades. By the mid-1980s, large parts of central and western Europe were affected. The westward expansion came to a halt in areas such as France and northern Italy, where foxes were treated with oral rabies vaccine. Infected foxes are responsible for maintaining the rabies virus within the fox population and also for transmission to other wildlife species and domestic animals. In affected areas, rabies is detected in a wide variety of species at different frequencies. To have an idea of what the rabies population dynamics look like, consider Figure 5.1 below. Here the data presented is from [24] and is comprised of all mammalian species in their database. For the data given below the observed infecteds, and dynamics are dominated by the observed infecteds of red foxes. Recall though, as previously mentioned, that the observations may only represent $2 - 10\%$ of the total number of infecteds. The data from many countries in Eastern and Western Europe is presented in [24], however as commonly noted, the Ukraine and the Russian Federation provide a reservoir for spreading the disease to other countries. The countries Belarus and Romania are also shown in Figure 5.1 to demonstrate the dynamics of countries near by.

Besides the dynamics presented above, there is also a variety of dynamics present within subpopulations. For instance observed cases within the human population present the dynamics in Figure 5.2.

Moving father from the Ukraine and the Russian Federation, we see that Western Europe is mostly free from rabies [1, 24]. They however are not free from the threat. Since fox rabies was eliminated from western Europe, the costs for oral vaccination have been substantially reduced but other European countries now striving to eliminate fox rabies are incurring high costs. Recent incursions into Italy, although now under control, required substantial financial commitments, and costs may escalate elsewhere, given the threat of emergence in rabies-free countries such as Greece. The

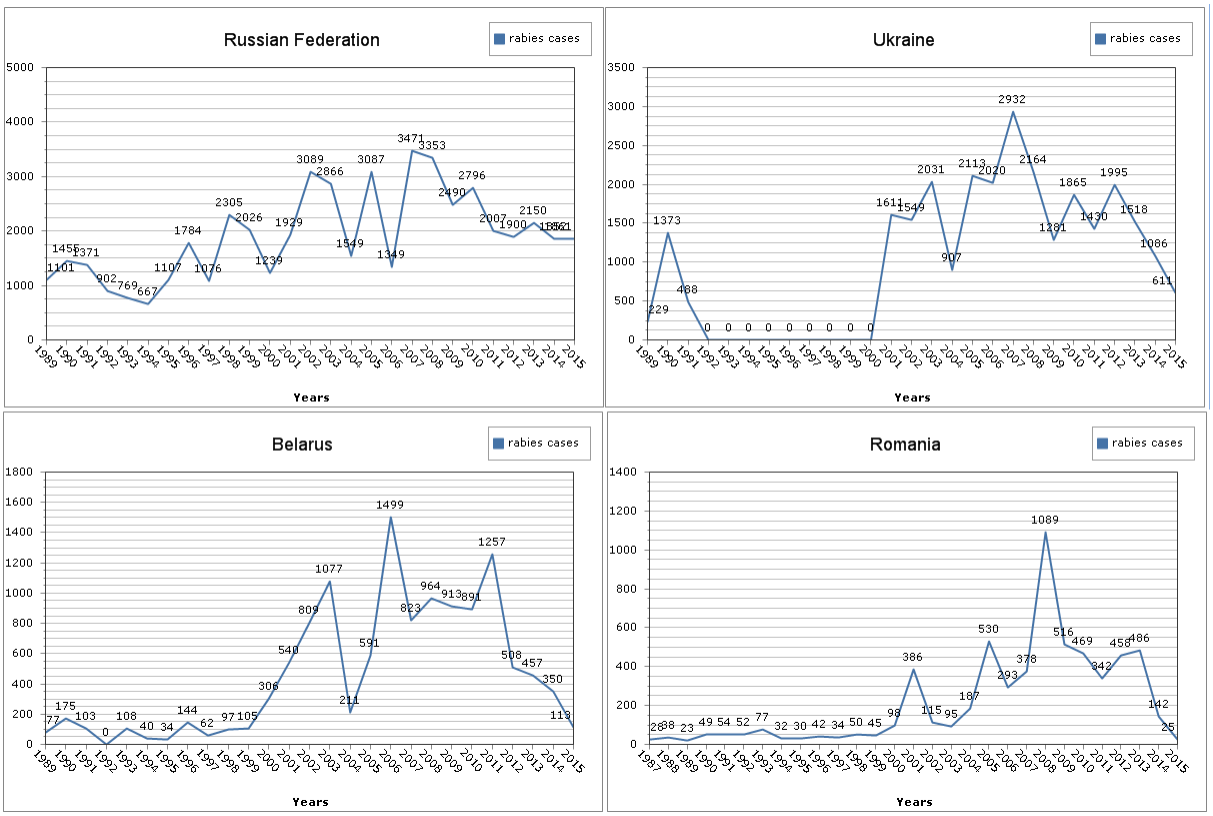

Figure 5.1: Number of Observed Cases on a yearly basis over all mammalian species. Data take from [24]

cost of setting up a protective barrier along the entire eastern border of the European Union to prevent such incursions is estimated to be over 6 million US dollars per year.

Consequently understanding the dynamics present in Easter Europe can be of value to Western Europe as well, allowing better and cheaper control strategies, such as mass vaccination which to date has been the most effective means of control [1].

The data from [24] seems to indicate that migration has pulse action (see Figure 5.1 and 5.2. We will start with the ODE given in [3] and modify it by allowing a periodic influx of infected individuals modeled as a pulse.

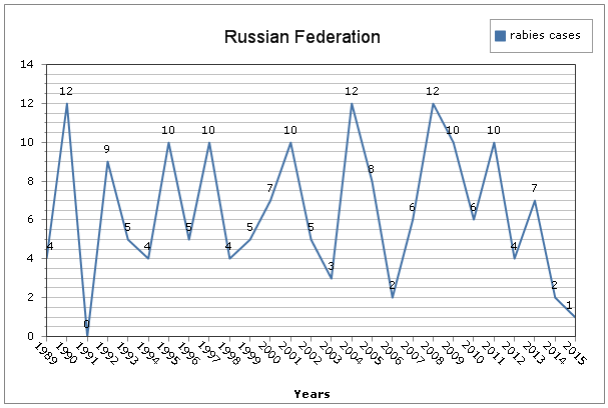

Figure 5.2: Number of Observed Cases of Rabies in Humans on a yearly basis. Data taken from [24]

5.3 MODEL

In this section first we review the model from [3] and then look to modify it by adding a discrete kick.

5.3.1 ODE

The model presented by [3] for modeling fox rabies in Europe is given by

$$[3]\begin{cases} \dfrac{dX}{dt} &= rX - \gamma XN - \beta XY \\ \dfrac{dI}{dt} &= \beta XY - (\sigma + b + \gamma N)I \\ \dfrac{dY}{dt} &= \sigma I - (\alpha + b + \gamma N)Y \end{cases} \tag{5.1}$$

- Number of Susceptible: X
- Number of Latent: I
- Number of Infected: Y
- Death Rate: b

- Population Growth Rate: a
- Latency Period: $1/\sigma$
- Death Rate of rabid foxes: α
- Rabies Transmission coefficient: β
- Self competition term related to carrying capacity: γ
- Immigration plus births - Emigration and deaths of susceptibles. γ

5.3.2 Adding Discrete Kicks to an ODE

Looking at the data in Figure 5.1 and 5.2 as well as from [24] there seems to be periodic pulses of infecteds. Consequently we will model this by modifying equation 5.1 above writing:

$$\begin{cases} \dfrac{dX}{dt} &= rX - \gamma XN - \beta XY \\ \dfrac{dI}{dt} &= \beta XY - (\sigma + b + \gamma N)I + \sum_{n=0}^{\infty} hX\delta(t - nk) \\ \dfrac{dY}{dt} &= \sigma I - (\alpha + b + \gamma N)Y \end{cases} \tag{5.2}$$

- Dirac distribution (see Math Preliminaries): δ
- Time of first instance where infected foxes enter population: k

The new term added to the equation is given by $\sum_{n=0}^{\infty} hX\delta(t - nk)$. Since the other terms in the expression for dI/dt are bounded on any bounded time interval we can ignore them for our purposes and just before the time $t = nk$ write

$$\frac{dI}{dt} = hX\delta(t - nk) \tag{5.3}$$

which is essentially saying that the change of latents over time is a linear function of the number of susceptibles in the population. The delta distribution acts as a forcing term making the change instantaneous. Since X is a continuous function, we can integrate this to have:

$$I_a = I_b + hX_b \tag{5.4}$$

- Number of latent immediately after kick or integration: I_a
- Number of latent immediately before kick or integration: I_b
- Number of susceptible immediately before kick or integration: X_b

For more precise details on the integration and interpretation of the delta distribution see the section on the Dirac Distribution under Mathematical Preliminaries and 4.6 with the following discussions.

Justification for the kick term in the form of (5.3) is essentially that the rate of change in the number of latent should be proportional to the number of susceptible. A linear relationship is considered to start simple and avoid over fitting. We consider the rate of change to be a function of the susceptibles because, in standard epidemic model, the susceptible population determines either partially or completely whether a disease will become an epidemic or die out [15]. Ideally we would be interested in the number of susceptibles of nearby populations and not the one being modeled. Consequently the assumption is made here that they are similar. Since we are considering instantaneous pulses, the Dirac distribution acts as a forcing function to accommodate this. Also the kick is added to the latent since infected die very quickly so it is assumed the kick is really the latent which are later observed as infectious. These ideas leave us with equation 5.3.

5.3.3 Model Dynamics

If we consider the map implied by the equations in (5.2) with the parameters in Table 5.1 we wind of with dynamics represented in Figures 5.3 and 5.4 below. The reasons for picking these parameters is that rabies is known to exhibit complex dynamics so the parameter space was explored to see if this model was capable of more than just cycles and fixed points. From the figures, the dynamics appear to be complex, as with rabies dynamics, which we would like to verify. To proceed with this verification will note that the map has a hyperbolic fixed point at $X = I = Y = 0$. If we calculate the Jacobian of the map about this saddle point numerically we find it has a one dimensional unstable manifold and a two dimensional stable manifold. The computed eigenvalues where approximately $5226.444750313, 0.000010130094$ and $1.4180067 \times 10^{-}8$ however for calculations two-hundred decimal places of precision were used. It may be helpful to note that ratio of the unstable to the stable eigenvalues were about 400 billion and 500 million respectively. Noting the eigenvalues is important not just in terms of identifying a saddle point but the differences in magnitudes indicate how costly a mistake with integration can be since the eigenvalues indicate how quickly points move along the stable and unstable manifolds in a neighborhood of the saddle point. Systems such as this are considered stiff and the usually approach is to use integration methods which are A-Stable. It is not my intention to cover the details of A-Stability, however, the basic idea is to explore the properties of an integration algorithm for a linear model often called the "toy model." If the region of convergence to 0 for the algorithm is sufficiently large for the product of the step size and the eigenvalue of the toy model, the algorithm is said to be A-stable. Unfortunately, all A-stable methods are implicit meaning integration involves solving systems of nonlinear equations. Taylor Integration which was used in this problem is an explicit method that is asymptotically A-stable, however, which suffices for our purposes [26].

β	σ	b	r	γ	h	k	α
65	21	1	10	10	7.1	23/28	13

Table 5.1: Parameter values for used of the model in (5.2)

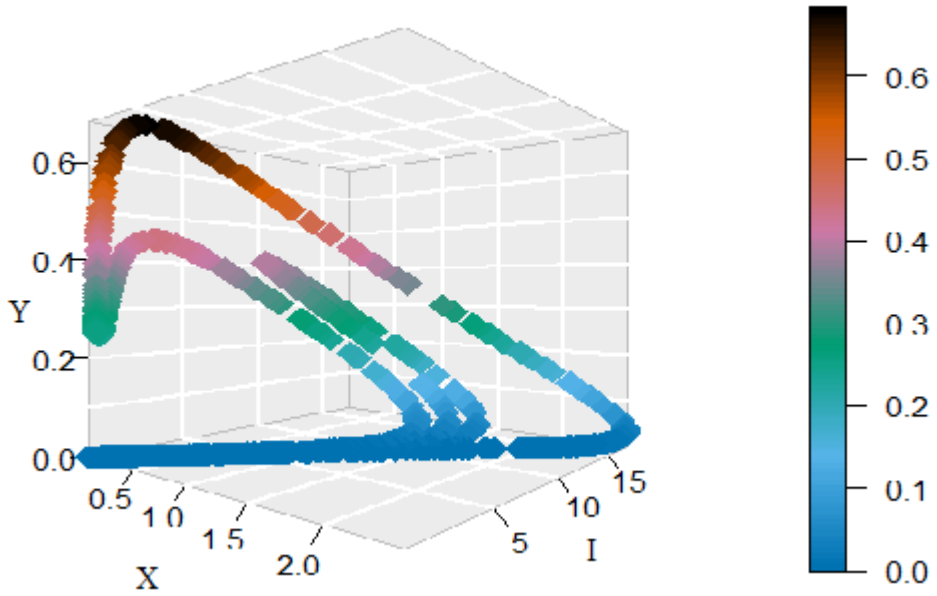

Figure 5.3: Plot of stroboscopic map defined in (5.2) with parameters defined at this beginning of this section.

5.4 ESTIMATING AN UNSTABLE MANIFOLD

In our rabies model our goal is to show the existence of a chaotic set. We do this by showing the transverse intersection of the stable and unstable manifolds for a fixed point, which results in the map represented by our model being conjugate to a horseshoe map and hence containing a chaotic set.

Since the maps we use in our models are implicit we take a numerical approach to estimate the stable and unstable manifolds. We begin by considering an analytic map $Q : \mathbb{R}^n \to \mathbb{R}^n$ and a saddle point p_0. The stable manifold theorem guarantees the existence of the local invariant stable and unstable analytic manifolds given by S and U respectively which are tangent to the stable and unstable spaces for $DQ(p_0)$

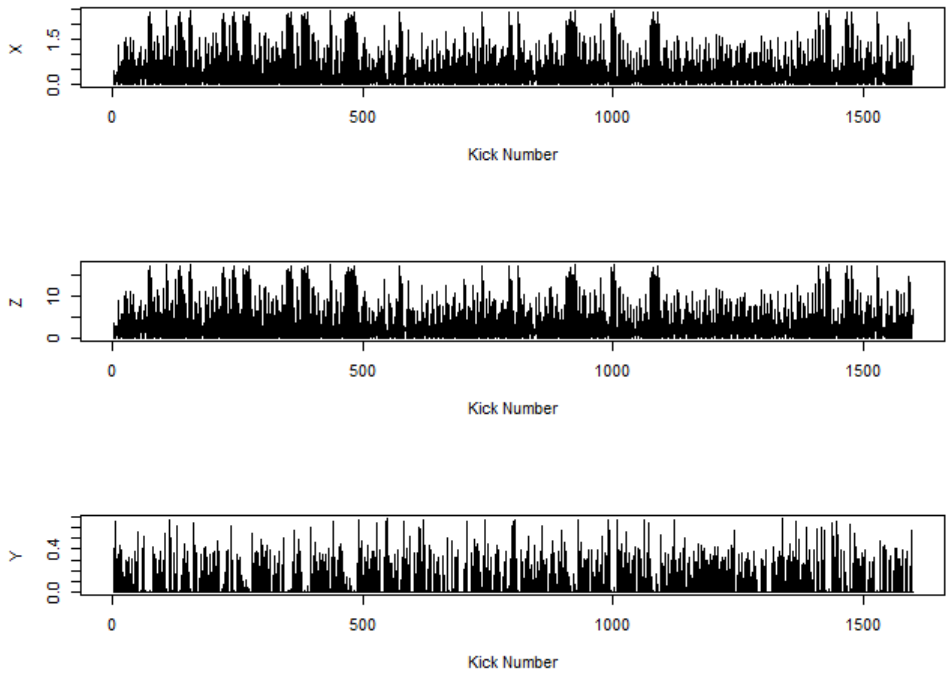

Figure 5.4: Times Series for stroboscopic map defined in (5.2) with parameters defined at the beginning of this section.

at the said point and of the same dimension. The global stable and unstable sets defined respectively below.

$$W^s(p_0) = \bigcup_{n\geq 0} Q^{-n}(S)$$

$$W^u(p_0) = \bigcup_{n\geq 0} Q^{n}(U)$$

We will discuss the procedure for estimating the unstable manifold, the procedure for the stable manifold is similar. As mentioned above suppose that the dimension of the unstable manifold is given by $k \leq n$. Then since the manifold is analytic it has a Taylor expansion about the point p_0. So we may parameterize W^u by Taylor expanding about a point $a \in \mathbb{R}^k$ as below.

$$\phi_\mu : \mathbb{R}^k \to \mathbb{R}^n$$

$$\phi_\mu(x) = p_0 + \sum_{|\alpha|\geq 1}^{\infty} \frac{(x-a)^\alpha}{\alpha!} \partial^\alpha \phi_\mu(a)$$

and

$$\phi_{N,\mu}(x) = p_0 + \sum_{|\alpha|\geq 1}^{N} \frac{(x-a)^\alpha}{\alpha!}\partial^\alpha \phi_\mu(a)$$

where

$$\alpha = (\alpha_1, \alpha_2, ..., \alpha_k)$$

$$|\alpha| = \alpha_1 + \alpha_2 + ... + \alpha_k$$

$$x = (x_1, x_2, ..., x_k)$$

$$x^\alpha = (x_1^{\alpha_1}, x_2^{\alpha_2}, ..., x_k^{\alpha_k})$$

$$\partial^\alpha = \partial^{\alpha_1}\partial^{\alpha_2}...\partial^{\alpha_k}$$

$$\partial_i^{\alpha_i} = \frac{\partial^{\alpha_i}}{\partial x_i^{\alpha_i}}$$

Using the above expansion about $a \in \mathbb{R}^k$, with $\phi_\mu(a) = p_0$, we may take a linear approximation and write

$$\phi_\mu(x) = p_0 + \partial\phi_\mu(x-a) + O((x-a)^2)$$

Since we know that ϕ_μ is locally tangent to the unstable eigenspace of $DQ(p_0)$, we may write

$$\phi_\mu(x) = p_0 + W(x-a) + O((x-a)^2) \tag{5.5}$$

where $W = [W_1, W_2, ..W_k]$ is a matrix of linearly independent columns and W_i is an unstable eigenvector of $DQ(S_u)$.

Providing a suitable expansion for the unstable manifold would mean knowledge of derivatives beyond the first order which we do not have. Consequently we will use the following property. Let $P_0 = \phi_\mu(x_0) \in W^u(p_0)$. Then we have that for any $m_0 \in \mathbb{N}$ and λ and eigenvalue of $DQ(p_0)$.

$$P_0 = \lim_{N\to\infty} Q^{m_0} \circ \phi_{N,\mu}(\lambda^{-m_0} x_0) \tag{5.6}$$

However convergence is faster when $\lambda^{-m_0} x_0 << 1$, which is the point we will exploit[7]. If Q were a linear map then ϕ_μ would just be a matrix consisting of the unstable eigenvectors of $DQ(p_0)$ and we could then think this of this as just the eigenvalue property. Then using a linearizion argument, as suggested here, or Normal Form theory we can show that this property holds locally even when Q is not linear. The property can then extended as a global property of the unstable manifold. To see why this property is useful note that λ gives us information about how quickly points move along the unstable manifold and since $\lambda = 1$ represents a non-hyperbolic case we would like to stay as far away from this as possible. Consequently we may be better off looking at the map Q^{m_0} and the eigenvalues λ^{m0} if they are more hyperbolic. However, since we are trying to estimate ϕ_μ this is just an asymptotic approximation as $\phi_{N,\mu} \to \phi_\mu$.

Specifically we will start with a small neighborhood B_0 of points about $0 \in \mathbb{R}^k$. We can then approximate where on the unstable manifold these points should be mapped using equation 5.6 above writing

$$W^u(p_0) \cong W^u_{N,m_0} = \{Q^{m_0} \circ \phi_{N,\mu}(\lambda^{-m_0} x_0) | \forall x_0 \in B_0\} \tag{5.7}$$

We can compute an initial linear approximation for $\phi_{0,\mu}$ and W^u_{0,m_0} using equation 5.5 then get a better approximation of the points for the unstable manifold using 5.6. We then fit W^u_{0,m_0} using least squares regression by a polynomial of the desired degree,

say N. Since the Taylor expansion of ϕ_μ is unique we expect that this regression will approximate $\phi_{N,\mu}$. Using our estimate of $\phi_{N,\mu}$ we may use equations 5.6 and 5.5 again to get a better estimate W^u_{N,m_0}. We repeat this process to show convergence of the polynomial coefficients for $\phi_{N,\mu}$.

5.5 RESULTS

Applying the algorithm in the previous section to our map we calculated parameterizations for the unstable and stable manifolds. For the unstable manifold the change in regression coefficients with respect to the L^2 norm is shown in Figure 5.5. Noting this is only a Cauchy argument, however, there does appear to be convergence. For the stable manifold only two iterations were performed. Integrating backwards in time was a computationally difficult task. For the current results 1000 terms were needed with the Taylor integration of the ODE part of 5.2. Using less terms results in nonsensical results or the system blowing up. Computation is expensive due to the convolutions products in the Taylor series. Recently work has been done to speed this up using cluster based computing. Concerning the Taylor expansion for the unstable manifold 200 terms were used in the expansion. Most of the terms converged quickly to 0, so the manifold could be fit with a polynomial of lesser degree. A large number of terms were used since Taylor expansions are infinite and if the algorithm is working the less important terms should tend to zero in any case. For the stable manifold only 30 terms were used do to time constraints resulting from computational difficulty.

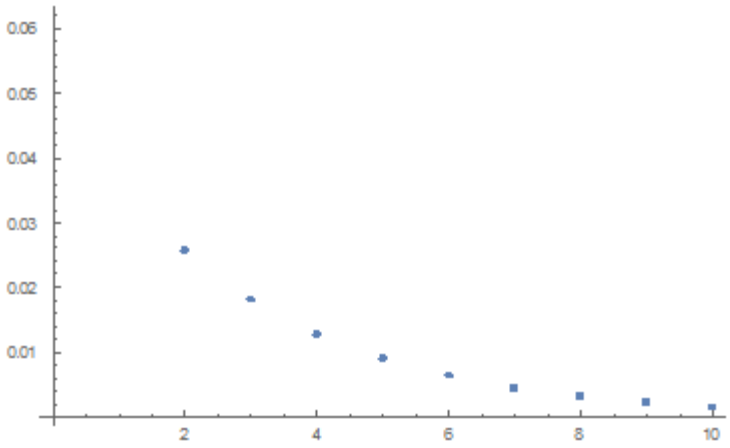

Figure 5.5: Considering polynomial fits for the unstable manifold with 200 terms, the above figure hows the change in the coefficients versus algorithm iteration under the L^2 norm.

The output of the algorithm can be viewed in Figure 5.6 below. The upper left and right show estimations of the stable and unstable manifolds respectively. The bottom center demonstrates their intersection which at least from the numerical approximations appears to be transverse indicating conjugacy to a horseshoe map and hence a chaotic set and addressing the question if the model from [3] can be modified to handle the more complex dynamics of rabies models.

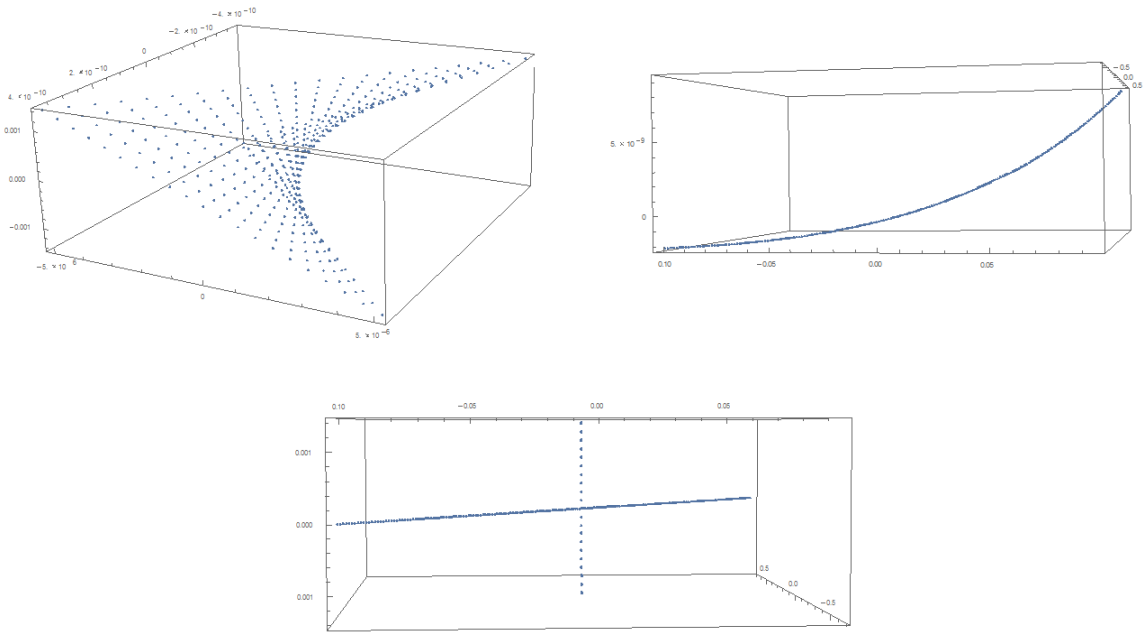

Figure 5.6: Stable and Unstable manifolds for the fixed point $(0, 0, 0)$. Upper lefts is an estimation of the stable manifold. Upper right is an estimation of unstable manifold. Bottom center is an overlay showing the intersection of the stable and unstable manifolds

5.6 DISCUSSION

As pointed out in the introduction for this chapter rabies is both a serious problem and one known to exhibit complex dynamics. In [3] a model was developed for the rabies virus and a variable population however the model leaves out migration events that are known to be important to rabies dynamics. For instance, dispersion of juveniles, increased contact during mating season etc. To account for what from the data seem to be impulse events and likely migration, as in the previous case study a Dirac distribution was used, and it was assumed to be a function of the number of suseptiables in the surrounding community. The assumption is made that the number of susceptibles in the community being modeled is proportional to the number of susceptibles in surrounding communities. Also it is known that epidemics tend to be driven by the number of susceptibles. Starting with a simple pulse to

avoid over fitting [2] we note for certain parameter ranges the existence of complex dynamics appearing to be chaotic. To verify this the algorithm in the previous section was used to estimate the stable and unstable manifolds and look at their intersection. After running the algorithm the estimations appear to have a transverse intersection. Unfortunately due to stiffness of the ode the accuracy of the manifolds was only computed to eight decimal places. The computation of this intersection is evidence that this model can mimic the complex dynamics found in nature.

With regards to the algorithm only eight digits of accuracy were attainable with the constraint seemingly due to computational restraints. The ratio of the eigenvalues for the unstable to the stable manifolds had an order as high as 4 billion meaning slight errors in the computations can blow up very quickly. Consequently expansions on the order of 1000 terms were used for Taylor Integration. This placed further restraints on the number of times the algorithm for estimating the manifolds could be used. For the unstable manifold expansion(not Taylor Integration) 200 terms were used and for the stable manifold 30 were used the latter case being two dimensional. Since the main difficulty in the calculation stems from integration of the underlying ODE a few modifications may be made here. One option would be to use a integrator other than Taylor's method. In this choice however we should recall that Taylor's method is asymptotically A-stable and A-stability is a desired property for stiff systems. Using another integrator would either involve very small step sizes, if not A-stable, while A-stable methods are implicit making implementation reliant on solving non-linear equations. Another option would be to parallelize the convolution product. Since the convolutions in the Taylor expansion for this system can be thought of as taking the dot product of one vector with the reverse of another vector this process can easily be split up among a cluster of computers or multiple cores.

BIBLIOGRAPHY

[1] WHO Expert Consultation on Rabies Second Report. Technical report, 2013.

[2] Peter A. Abramsemai and Lev R. Ginzburg. The nature of predation: prey dependent, ratio dependent or neither. *Trends in Ecology and Evolution*, 15:337–341, 9 2000.

[3] Roy M Anderson, Helen C. Jackson, Robert M. May, and Anthony M. Smith. Population dynamics of fox rabies europe. *Nature*, 289(26):765–771, 1981.

[4] RB Aronson and WF Precht. Stasis, biological disturbance, and community structure of a holocene coral reef. *Paleobiology*, 23(3):326–346, 1997.

[5] J. Blackwood, A. Hastings, and P.Mumby. A model-based approach to determine the long-term effects of multiple interacting stressors on coral reefs. *Ecological Applications*, 21(7):2722–2733, 2011.

[6] Carmen Chicone. *Ordinary Differential Equations with Applications*. Springer, New York, NY, 2006.

[7] V. Gilfreich and V. Naudot. Width of the homoclinic zone in the parameter space for quadratic maps. *Experimental Mathematics*, 18(4):409–427, 1 2011.

[8] Nicholas AJ Graham, David R Bellwood, Joshua E Cinner, Terry P Hughes, Albert V Norström, and Magnus Nyström. Managing resilience to reverse phase shifts in coral reefs. *Front Ecol Environ*, 11:541–548, 2013.

[9] J.F. Heagy. A physical interpretation of the henon map. *Physica D*, 57:436–446, 1992.

[10] Katja Holmana and Kaarina Kauhala. Ecology of wildlife rabies in europe. *Mammal Review*, 36(1):17–36, 2006.

[11] T. P. Hughes, A. H. Baird, D. R. Bellwood, M. Card, S. R. Connolly, C. Folke, R. Grosberg, O. Hoegh-Guldberg, J. B. C. Jackson, J. Kleypas, J. M. Lough, P. Marshall, M. Nyström, S. R. Palumbi, J. M. Pandolfi, B. Rosen, and J. Roughgarden. Climate change, human impacts, and the resilience of coral reefs. *Science*, 301:929–933, 2003.

[12] Terence P. Hughes. Catastrophies, phase shifts, and large-scale degradation of a caribbean coralreef. *Science*, 265(5178):1547–1551, 9 1994.

[13] Terence P. Hughes, Daniel C. Reed, and Mary-Jo Boyle. Herbivory on coral reefs: community structure following mass mortalities of sea urchins. *Exp. Mar. Biol. Ecol*, 113(1):39–59, 1987.

[14] Jeremy Jackson, Katie Cramer, Mary Donovan, Alen Friedlander, Andy Hooten, and Jean-Marc Lam, Vivian Jézéquel. Coral reef resilience workshop report. Panama City, Republic of Panama, April -May 2012. GCRMN.

[15] Matt J. Keeling and Pejman Rohani. *Modeling Infectious Diseases*. Princeton University Press, New Jersey, 2008.

[16] Nancy Knowlton. Thresholds and multiple stable states in coral reef community dynamics. *American Zoologist*, 32(6):674–682, 1992.

[17] Bruce Kusse and Eric Westwig. *Mathematical Physics*. John Wiley and Sons,inc, New York, 1998.

[18] Robert M Martini, Joao P Krajewski, Cristina Sazima, and Ivan Sazima. Foraging activity and resource use by three parrotfish species at Fernando de Noronha Archipelago, tropical west atlantic. *Marine Biology*, 149:423–433, 2006.

[19] R. P. M.Bak, M. J. E. Carpay, and E. D. de Ruyter van Steveninck. Density of the sea urchin *Diadema antillarum* before and after mass mortalities on the coral reefs of Curaao. *Mar. Ecol. Prog. Ser*, 17:105–108, 1984.

[20] TR McClanahan, V Hendrickn, and MJ Rodrigues. Varying responses of herbivorous and invertebrate- feeding fishes to macroalgal reduction on a coral reef. *Coral Reefs*, 18:195–203, 1999.

[21] Peter J. Mumby. Phase shifts and the stability of macroalgal communities on Caribbean coral reefs. *Coral Reefs*, 28:761–773, May 2009.

[22] Peter J. Mumby, Alan Hastings, and Helen J. Edwards. Thresholds and the resilience of caribbean coral reefs. *Nature*, 450(1):98–101, 11 2007.

[23] William W. Murdoch, Cheryl J. Briggs, and Roger M. Nisbet. *Consumer-Resource Dynamics*. Princeton University Press, New Jersey, 2003.

[24] World Health Organization. Rabies information system of the WHO collaboration centre for rabies surveillance and research, 2014.

[25] Lawrence Perko. *Differential Equations and Dynamical Systems Third Edition*. Springer, New York, NY, 2001.

[26] Alfio Quarteroni, Richard Sacco, and Fausto Saleri. *Numerical Mathematics Second Edition*. Springer, Milan, 2006.

[27] Sidney Resnik. *A Probability Path*. Birkhauser, Boston, 2005.

[28] Clark Robinson. *Dynamical Systems Stability, Symbolic Dynamics and Chaos Second Edition.* CRC Press, Boca Raton, FL, 1999.

[29] MJ Shulman and D.R. Robertson. Changes in the coral reefs of San Blas, Caribbean Panama: 1983 to 1990. *Coral Reefs*, 15:231–236, 1996.

[30] Ray T. Sternera and Graham C. Smith. Modelling wildlife rabies: Transmission, economics, and conservation. *Science Direct*, June 2006.

[31] EHJ Williams and L Bunkley-Williams. The world-wide coral reef bleaching cycle and related sources of coral mortality. *Atoll Res Bull*, 355:1–72, 1990.

[32] Ivor D. Williams and Polunin. Large-scale associations between macroalgal cover and grazer biomass on mid-depth reefs in the Caribbean. *Coral Reefs*, 19:358–366, 2001.

[33] Ivor D. Williams, Nicholas V. C. Polunin, and Vicki J. Hendrick. Limits to grazing by herbivorous fishes and the impact of low coral cover on macroalgal abundance on a coral reef in Belize. *Marine Ecology Progress Series*, 222:187–196, 2001.

[34] Simon N. Wood. Partially specified ecological models. *Ecological Monographs*, 71(1):1–25, 2001.